

1 **Phosphoglycerol-type wall- and lipoteichoic acids are enantiomeric polymers**
2 **differentially cleaved by the stereospecific glycerophosphodiesterase GlpQ**

3
4 **Axel Walter¹, Sandra Unsleber¹, Jeanine Rismondo^{3#}, Ana Maria Jorge², Andreas Peschel²,**
5 **Angelika Gründling³, Christoph Mayer^{1*}**

6
7 ¹Microbiology/Glycobiology and ²Infection Biology, Interfaculty Institute of Microbiology and Infection
8 Medicine Tübingen (IMIT), University of Tübingen, Tübingen, Germany, ³Section of Molecular
9 Microbiology and Medical Research Council Centre for Molecular Bacteriology and Infection, Imperial
10 College London, United Kingdom

11
12 Running title: *stereochemistry of teichoic acids*

13
14 [#]Present address: Department of General Microbiology, GZMB, Georg-August-Universität Göttingen,
15 37077 Göttingen, Germany

16 ^{*}To whom correspondence should be addressed: Christoph Mayer: Interfaculty Institute of Microbiology
17 and Infection Medicine Tübingen (IMIT), Microbiology/Glycobiology, University of Tübingen, Auf der
18 Morgenstelle 28, 72076 Tübingen, Germany: christoph.mayer@uni-tuebingen.de; Tel. +49 (7071) 29-
19 74645.

20
21 **Keywords:** teichoic acids, WTA, LTA, teichoicase, glycerol-phosphate, stereochemistry

22
23 Title: 151 characters

24 Words for the abstract: 250

25 Words for the text: 10679

26
27 **ABSTRACT**

28 The cell envelope of Gram-positive bacteria generally comprises two types of polyanionic polymers, either
29 linked to peptidoglycan, wall teichoic acids (WTA), or to membrane glycolipids, lipoteichoic acids (LTA).
30 In some bacteria, including *Bacillus subtilis* strain 168, WTA and LTA both are glycerolphosphate
31 polymers, yet are synthesized by different pathways and have distinct, although not entirely understood
32 morphogenetic functions during cell elongation and division. We show here that the exo-lytic *sn*-glycerol-
33 3-phosphodiesterase GlpQ can discriminate between *B. subtilis* WTA and LTA polymers. GlpQ
34 completely degrades WTA, lacking modifications at the glycerol residues, by sequentially removing

35 glycerolphosphates from the free end of the polymer up to the peptidoglycan linker. In contrast, GlpQ is
36 unable to cleave unmodified LTA. LTA can only be hydrolyzed by GlpQ when the polymer is partially
37 pre-cleaved, thereby allowing GlpQ to get access to the end of the polymer that is usually protected by a
38 connection to the lipid anchor. This indicates that WTA and LTA are enantiomeric polymers: WTA is
39 made of *sn*-glycerol-3-phosphate and LTA is made of *sn*-glycerol-1-phosphate. Differences in
40 stereochemistry between WTA and LTA were assumed based on differences in biosynthesis precursors
41 and chemical degradation products, but so far had not been demonstrated directly by differential,
42 enantioselective cleavage of isolated polymers. The discriminative stereochemistry impacts the dissimilar
43 physiological and immunogenic properties of WTA and LTA and enables independent degradation of the
44 polymers, while appearing in the same location; e.g. under phosphate limitation, *B. subtilis* 168 specifically
45 hydrolyzes WTA and synthesizes phosphate-free teichuronic acids in exchange.

46

47 **Introduction**

48 Bacteria are covered by a complex multilayered cell envelope positioned external to the cell membrane,
49 which protects the susceptible protoplast from detrimental effects of the environment and the cells from
50 lysis (1). Differences within the composition of the cell envelope classifies the two major groups of
51 bacteria, Gram-negatives and Gram-positives. Gram-negative bacteria are encased in a thin peptidoglycan
52 (PGN) layer that is covered by an external outer membrane (OM), carrying negatively charged
53 lipopolysaccharide (LPS) in the outer leaflet. In contrast, Gram-positive bacteria lack an OM, but possess
54 a thick PGN layer that is interweaved by polyanionic glycopolymers, the teichoic acids, which were
55 discovered by Baddiley and coworkers 60 years ago (2-4). Teichoic acids can be very variable in
56 composition and structure, although they mostly feature glycerol-phosphate, ribitol-phosphate, or sugar
57 phosphate repeating units connected through phosphodiester bonds (5-8). These phosphodiester-polymers
58 are either covalently bound to the PGN and called wall teichoic acids (WTA) or linked to membrane
59 glycolipids, anchored in the cell membrane and named lipoteichoic acids (LTA) (4,9,10). WTA are
60 characteristic constituents of the Gram-positive cell walls (PGN-WTA complex), comprising chains of 30
61 to 50 polyol-phosphate repeats, connected via phosphodiester and anchored via a linker disaccharide (*N*-
62 acetylmannosamine- β -1,4-*N*-acetylglucosamine; ManNAc- β -1,4-GlcNAc) to about every ninth *N*-
63 acetylmuramic acid (MurNAc) residue of the PGN (9). They make up about half of the cell wall dry weight
64 (11,12) and are responsible for the generally high phosphate content of Gram-positive cell walls (4,13). It
65 was shown that WTA can serve as phosphate storage, allowing *B. subtilis* to continue growth under
66 phosphate-depleted conditions (13-15). Under these conditions, teichoic acids are exchanged with
67 phosphate-free teichuronic acids to cope with this stress, which is an adaptation process known as the
68 “teichoic acid-to-teichuronic acid switch”. LTA is more widespread in bacteria than WTA and the

69 composition is less dependent on growth conditions (16). Commonly, LTA contain polyol-phosphate
70 chains (Type I LTA) that are anchored in the cytoplasmic membrane via glycolipids; in the case of *B.*
71 *subtilis*, a gentibiosyl disaccharide (glucose- β -1,6-glucose) glycosidically bound to diacylglycerol (10).
72 Although differences in the chemical composition, route of biosynthesis, as well as roles in cell growth
73 and morphogenesis have been identified between WTA and LTA, their physiological functions are still
74 insufficiently understood (4,17-19). Inactivation of both LTA and WTA is lethal in *B. subtilis*, indicating
75 partially redundant functions, nevertheless comparison of the individual mutants suggested that they have
76 distinct roles during cell elongation (WTA) and division (LTA) (18). Further proposed functions of teichoic
77 acids include control of cell wall targeting enzymes during envelope homeostasis and divalent cation
78 binding (3,20), interaction with host and bacteriophage receptors (18,21), as well as pathogenicity (22-24).
79 Recently, LTA has been suggested to functionally resembling the osmoregulated periplasmic glycans of
80 Gram-negative bacteria (10,25,26).

81 In some Gram-positive bacteria, including *B. subtilis* 168 as well as in *S. epidermidis* and *S.*
82 *lugdunensis*, both LTA and WTA are glycerophosphate polymers (17,18,27,28). Nevertheless, they are
83 synthesized by distinct routes (9,10,29). Figure 1 summarizes the biosynthesis pathways of WTA and LTA
84 of *B. subtilis* 168. WTA is synthesized from CDP-glycerol in the cytoplasm and the polymer is then flipped
85 outwards (Fig. 1A). In contrast, LTA is synthesized from the precursor phosphatidylglycerol (PG),
86 generated via diacylglycerol(DAG)-CDP and PG-phosphate (PGP). The PG precursor is subsequently
87 translocated and then polymerized on the outside of the cell (Fig. 1B). An important finding has been that
88 the glycerophosphate in the precursors of WTA and LTA have different stereochemistry (17). CDP-
89 glycerol has a *sn*-3-configuration, and in contrast to this, the free glycerol phosphate of PG has a *sn*-1-
90 configuration. The prochirality of glycerol leads to two 3-phosphate products: according to convention
91 (stereochemical numbering: *sn*-nomenclature), L-glycerol is the configuration that determines the
92 numbering of *sn*-glycerol phosphates (Fig. 1C). The use of different precursors and the
93 compartmentalization of WTA and LTA synthesis allows to differentially regulate the production of the
94 two polymers, which is important in order to fulfil particular roles in cell envelope integrity and distinct
95 morphogenetic functions during cell cycle and growth phases (18). In contrast, how WTA and LTA execute
96 their distinct physiological functions is not obvious, as they are both present in the same cell envelope
97 compartment.

98 Modifications of the polyols by alanylation and glycosylation are important means to alter the
99 physiological properties of WTA and LTA and also affect recognition by the innate immune system
100 (6,30,31). D-alanylation adds positive charge (free amino groups) to the polyol-phosphate polymers,
101 thereby rendering the anionic character and as a consequence the binding properties (10,32). The
102 multienzyme complex DltABCD is responsible for adding D-Ala modifications onto LTA on the outer

103 leaflet of the cell membrane, and indirectly also onto WTA (Fig. 1) (32-35). LTA and WTA can also be
104 α -, or β -glycosylated, which severely increases the stability of these polymers against alkaline hydrolysis
105 (9,10). In *B. subtilis* the enzyme TagE transfers α -glucosyl residues from UDP-glucose onto preformed
106 WTA within the cytoplasm and constitutes the only WTA glycosylating enzyme in this bacterium (Fig.
107 1A) (36,37). Although WTA glycosylation usually occurs prior to the translocation of the polymer across
108 the cell membrane, it was recently proposed that it may also occur after translocation in *Listeria*
109 *monocytogenes* (37,38). Alike alanylation, glycosylation of LTA generally occurs, along with synthesis,
110 outside the cell, and membrane associated three component glycosylation systems responsible for LTA
111 glycosylation have been characterized recently in *B. subtilis* and *S. aureus* (CsbB/GtcA/YfhO) as well as
112 in *L. monocytogenes* (GtlA/GtlB) (Fig. 1B) (38-40).

113 Besides synthesis, also the turnover of WTA and LTA needs to be differentially regulated, which
114 so far has not been explored in much detail. Recently, the exo-acting *sn*-glycero-3-phosphate
115 phosphodiesterase GlpQ, along with an endo-acting phosphodiesterase PhoD, has been implicated in the
116 degradation of WTA during phosphate starvation (41). However, apart from WTA degradation during
117 adaptation to phosphate starvation, turnover of WTA likely occurs also along with the turnover of PGN of
118 the cell wall in *B. subtilis* and other Gram-positive bacteria (42-44). Since strains of *B. subtilis* lacking
119 both WTA and LTA are not viable, the simultaneous degradation of both polymers would be detrimental
120 (18). We thus wondered how differential degradation of WTA and LTA by hydrolases (“teichoicases”) is
121 possible. Previous studies with the glycerophosphodiesterase GlpQ of *B. subtilis* as well as orthologous
122 enzymes from *Escherichia coli* and *S. aureus* (amino acid sequence identities of 29 and 54 %, respectively)
123 have revealed strict stereospecificity for glycerophosphodiesteres harbouring *sn*-glycerol-3-phosphoryl
124 groups, e.g. produced by phospholipases from membrane phospholipids (41,45-47). Accordingly,
125 phosphatidylglycerol or lysophosphatidylglycerol, which harbour only free *sn*-glycerol-1-phosphoryl ends
126 are not hydrolyzed by GlpQ and also bis(*p*-nitrophenyl)-phosphate, a chromogenic substrate for other
127 phosphodiesterases, is not cleaved by GlpQ (45,46). Intriguingly, LTA of *S. aureus* was found to be not a
128 substrate of GlpQ, which however could be due to phosphoglycerol backbone modifications (47). In
129 contrast, the enzyme shows broad substrate specificity with respect to the alcohol moiety and can hydrolyse
130 a variety of different phospholipid head groups, such as glycerophosphocholine,
131 glycerophosphoethanolamine, glycerophosphoglycerol, and bis(glycerophospho)glycerol (41,45,47).

132 So far, differential cleavage of WTA and LTA polymers by GlpQ has not been examined in detail.
133 In this work, we show that the stereospecific *sn*-glycerol-3P phosphodiesterase GlpQ acts as an exo-lytic
134 hydrolase that sequentially cleaves off *sn*-glycerol-3-phosphate (Gro3P) entities from the exposed end of
135 WTA, however, it is unable to hydrolyse intact LTA. Thereby we provide biochemical evidence that these
136 polymers have opposite stereochemistry: WTA constitute phosphodiester-polymers made of Gro3P and

137 LTA polymers of *sn*-glycerol-1-phosphate (Gro1P). The stereochemical difference likely impacts many of
138 the polymers' distinct properties, such as interactions with hydrolases and binding of proteins throughout
139 the cell cycle, bacterial growth and differentiation.

140

141 RESULTS AND DISCUSSION

142 GlpQ is a stereospecific *sn*-glycerol-3-phosphoryl phosphodiesterase

143 GlpQ of *B. subtilis* and orthologs from other bacteria have been shown previously to specifically release
144 Gro3P from GPC, glycerophosphoethanolamine, glycerophosphoglycerol, and bis(glycerophospho)
145 glycerol. For the latter two substrates, K_M and k_{cat} values of 1.0 mM and 1275 min⁻¹, respectively 1.4 mM
146 and 1517 min⁻¹, were determined for *B. subtilis* GlpQ (41,45,47). We confirmed the stereospecificity of
147 recombinantly expressed, *B. subtilis* GlpQ for *sn*-glycero-3-phosphoryl substrates and determined the
148 enzyme's stability and catalytic optima, using *sn*-glycero-3-phosphocholine (GPC) as substrate
149 (Supporting Information, Fig. S1). Our analysis revealed that GlpQ is rather temperature sensitive. It
150 readily loses stability at temperatures above 30°C, e.g. within 30 min at 37°C more than 50% of its activity
151 was lost. At the same time however, the enzymatic turnover steadily increases with temperature up to an
152 optimum at 55°C and about half maximum activity at 30°C (Supporting Information, Fig. S1B).
153 Furthermore, the enzyme was shown to be stable over a remarkably wide pH range between 2 to 10, but
154 has a very narrow optimum at pH 8.0 (Supporting Information, Fig. S1B). We thus conducted all
155 experiments with the enzyme GlpQ in this study at 30°C and pH 8.0.

156 Although the detailed mechanism of phosphodiester-cleavage by GlpQ is currently unknown, Ca²⁺
157 ions were recognized as crucial for catalytic activity (yet they can be substituted with Cd²⁺ and partially
158 with Mn²⁺ and Cu²⁺) (45,48). Accordingly, the catalytic reaction was inhibited with
159 ethylenediaminetetraacetic acid (EDTA). Nevertheless the addition of Ca²⁺ ions was not required when
160 using the recombinant GlpQ that was purified from the cytosolic extracts of *E. coli*. The recently solved
161 crystal structure of the *B. subtilis* GlpQ with Gro3P bound to the active site (structural database identifiers:
162 5T9B and 5T9C) confirmed the importance of a Ca²⁺ ion for catalysis as well as for the stereospecific
163 coordination of the substrate (41,48). The active site of GlpQ includes a residue (His85) that is located on
164 a small additional, so-called glycerophosphodiester phosphodiesterase domain, which is inserted between
165 the beta-strand and alpha-helix of the second beta/alpha motif of a classical triose phosphate isomerase
166 (TIM)-barrel structure (41,49). Figure 2 depicts the substrate and Ca²⁺ binding sites of GlpQ, located in a
167 deep pocket located on the TIM barrel domain, and rationalizes the strict stereospecificity of the enzyme.
168 The substrate binding cleft can be divided into a hydrophilic side including the active site Ca²⁺ ion and a
169 hydrophobic side consisting of hydrophobic amino acids including phenylalanine and tyrosine (Phe190,
170 Tyr259, Phe279) (Fig. 2). The active site Ca²⁺ ion adopts a pentagonal bipyramidal coordination. It is held

171 in place by glutamic and aspartic acid residues (Glu70, Glu152, Asp72) and is also coordinated by the two
172 hydroxyl groups of Gro3P (Fig. 2). The phosphate as well as the C2 and C3 hydroxyl-group of Gro-3P are
173 drawn towards the active site Ca^{2+} ion, and are moved away from the hydrophobic side of the binding cleft.
174 Coordination of the Ca^{2+} ion by amino acids with charged side chains and the hydroxyl and phosphate
175 groups of the substrate as well as the orientation of the hydrophobic C-H groups of the substrate towards
176 the hydrophobic side of the binding cleft restricts the productive binding to the unsubstituted *sn*-glycero-
177 3-phosphoryl stereoisomer, thus allowing productive binding only of *sn*-glycerol-3-phosphoryl groups.
178 Instead, the C2 hydroxyl group of *sn*-glycerol-1-phosphoryl would face towards the hydrophobic side,
179 making the binding impossible. The hydrophilic side of the binding cleft also coordinates the phosphate
180 group of the substrate involving the basic side chains of His43, Arg44, His85 (Fig. 2). His43 and His85
181 presumably are functioning as general acid and base residues in the mechanism of phosphodiester
182 hydrolysis (48). The proposed catalytic mechanism of GlpQ involves the anchimeric assistance of the C2
183 hydroxyl group, thus requiring this group to be unmodified (i.e. not glycosylated or alanylated at the C2
184 hydroxyl group of GroP) (41).

185

186 **GlpQ sequentially cleaves unmodified WTA by an exo-lytic mechanism**

187 The glycerophosphodiesterase GlpQ of *B. subtilis* has been identified recently as a teichoicase that
188 preferentially digests polyGroP-type WTA lacking modifications on the glycerol subunits (41). However,
189 in this study, product formation with GlpQ had not been followed using polymeric teichoic acids as
190 substrates and thus, neither the strict specificity for unmodified WTA nor the exo-lytic mechanism have
191 been unequivocally shown. We thus aimed at directly monitoring product release by GlpQ from cell wall
192 (PGN-WTA complex) preparations using high performance liquid chromatography-mass spectrometry
193 (HPLC-MS). We first applied cell wall preparations containing glycosylated WTA, which were extracted
194 from *B. subtilis* 168 wild-type cells, and cell wall preparations containing non-glycosylated WTA, which
195 were extracted from $\Delta tagE::erm$ cells lacking the WTA alpha-glucosyl transferase TagE (cf. Fig. 1). These
196 samples were digested with GlpQ and product formation was followed by HPLC-MS; Figure 3 depicts the
197 base peak chromatograms (BPC), indicating the total ions in the sample preparations, and the extracted ion
198 chromatograms (EIC) in positive ion mode with $(M+H)^+ = 173.022$ m/z, which is the exact mass for GroP,
199 shown in blue. In both cell wall samples, either extracted from wild-type or $\Delta tagE::erm$ cells, no GroP
200 was detected in the absence of GlpQ, while upon incubation with the enzyme GroP is released (Fig. 3).
201 Whereas GlpQ releases large amounts of GroP from cell wall samples from $\Delta tagE::erm$ cells containing
202 unmodified WTA, and only very little amounts of GroP from glycosylated WTA extracted from wild-type
203 cells (Fig. 3). The amounts of GroP, determined by calculating the area under the curves (AUC), were
204 about 22 times higher when applying cell walls containing unglycosylated WTA ($\text{AUC} = 5.9 \times 10^6$)

205 compared to cell walls containing glycosylated WTA prepared from wild-type cells ($AUC = 2.7 \times 10^5$),
206 which is in agreement with the proposed chain length of the WTA polymers of 30 - 50 polyol-phosphate
207 repeats. The identity of the GroP reaction product was confirmed by MS and the spectra revealed typical
208 adduct pattern and isotope profiles for GroP (Supporting Information, Fig. S2A). It should be noted that
209 with the HPLC-MS method, it is not possible to distinguish between the two stereoisomers of GroP (cf.
210 Fig. 1C). However, given the strict stereospecificity of GlpQ, the product of WTA cleavage has to be *sn*-
211 glycerol-3-phosphate. Very little GroP is released from cell walls containing glycosylated WTA (compare
212 Fig. 3C and D), thus we suggest that GlpQ releases small amounts of non-glycosylated GroP from the free
213 ends of the substrate and stops when encountering a glycosylated (or alanylated) GroP in the chain
214 polymer. Only GroP without modification is released from WTA with GlpQ and no other possible
215 products, neither GroP-Glc, GroP-Ala and other glycosylated or alanylated products, nor larger polymeric
216 products could be detected by HPLC-MS. Thus, GlpQ can be classified as a teichoicase that specifically
217 hydrolyses unmodified *sn*-glycero-3-phosphoryl-WTA.

218 D-Ala substitutions were removed in the teichoic acid samples by pretreatment as well as applying
219 the GlpQ reaction at pH 8. It has been reported earlier that alanyl esters are rather labile at pH >7, with a
220 half time of hydrolysis at pH 8 and 37°C of 3.9 h (32,50). Accordingly, no difference in the release of GroP
221 was observed, when non-treated and pH 8-pretreated the WTA samples were compared (data not shown).
222 Furthermore, in a time course experiment we observed that already after a few seconds the majority of the
223 product of wild-type and unglycosylated (from *AtagE* cells) substrate is released by GlpQ (Supporting
224 Information, Fig. S3). Moreover, the amount of GroP released from from unglycosylated substrate did not
225 increase over time (over 2 h of incubation) and remained 22-fold higher than the product released from the
226 wild-type substrate. This indicates that GlpQ has only exo- and no endo-lytic activity and stops when a
227 glycosylated (or alanylated) GroP appears at the free end of the polymer, protecting the rest of the chain
228 from further digestion.

229 A complete digest of WTA by GlpQ should remove all GroP residues up to the linker disaccharide
230 ManNAc-GlcNAc. To show that this indeed occurs, cell wall preparations (PGN-WTA complex) were
231 thoroughly digested by GlpQ. As the enzyme is rather unstable, GlpQ was added repeatedly: after each
232 round of enzymatic digest for 10 min at 30°C, the supernatant was checked for GroP release by HPLC-
233 MS and then new GlpQ enzyme was added until only very minor additional amounts of GroP were
234 detected. These exhaustively digested cell wall samples were then treated with 5% TCA for 2h at 60°C,
235 whereby the glycosidic phosphodiester bond connecting the WTA linker with the PGN was cleaved. The
236 release of the linker disaccharide was analyzed by HPLC-MS after neutralization of the sample. The
237 identity of the linker disaccharide was confirmed by a mass spectrum revealing typical fragmentations
238 (loss of water), sodium and potassium ion adducts and ¹³C-isotope pattern (Supporting Information, Fig.

239 **S2B**). As control, a complete chemical digest of the PGN-WTA complex was achieved by treatment with
240 0.5 M NaOH for 2h at 60°C in order to completely remove the GroP chain polymer. Subsequently, the
241 linker disaccharide was released from the latter samples by TCA treatment and analyzed by HPLC-MS.
242 The linker disaccharide was obtained from both wild-type and unglycosylated PGN-WTA complexes by
243 chemical digestion in equal amounts as shown in **Figure 4A and B**. The amount of linker disaccharide
244 released by chemical digestion was set as to 100% of linker disaccharide in the substrate. As another
245 control, the PGN-WTA complex was treated with TCA alone to determine the amounts of linker
246 disaccharide that TCA can release without requiring NaOH pretreatment. Very small amounts of linker
247 disaccharide (ca. 3.6% of the total) were released from both PGN-WTA variants (**Fig. 4C and D**). The
248 difference, however, becomes significant once the substrate was pre-digested with GlpQ. While from the
249 wild-type PGN-WTA no more linker was released with GlpQ than with TCA treatment alone, GlpQ was
250 able to digest about 60% of the WTAs up to the linker in the cell wall sample derived from *tagE* mutant
251 cells (**Fig. 4E and F**).

252 **GlpQ cleaves unmodified LTA only after pre-digestion**

253 Since GlpQ specifically cleaves unglycosylated WTA, we next wanted to investigate if also unglycosylated
254 LTA can act as a substrate of the enzyme. Recently the glycosyltransferase CsbB has been shown to be
255 required for glycosylation of LTA in *B. subtilis* (38). LTA was purified from *B. subtilis* wild-type and
256 $\Delta csbB::kan$ cells using established protocols (51,52). Since LTA has been reported to be extensively
257 modified by D-alanyl esters, we aimed to remove also these modifications prior to GlpQ treatment. In a
258 previous study, it has been shown that incubation of LTA at pH 8.5 for 24 h at room temperature leads to
259 an almost complete removal of D-alanyl esters (22). However, according to these data, also partial
260 degradation occurs during this treatment, albeit the degradation apparently is very limited (the degree of
261 polymerisation dropped from 48 to 43). Since we wanted to avoid absolutely any degradation of the LTA
262 samples, we decided to apply slightly milder conditions, and thus preincubated the LTA preparations in
263 borate buffer at pH 8 for 24 h. The removal of alanine modifications was controlled by NMR (**Supporting**
264 **Information, Fig. S4**). ¹H-NMR spectra of LTA showed characteristic resonances corresponding to D-
265 alanyl ester modifications: signal at $\delta = 5.35, 4.20$ and 1.64 ppm and 4.2 ppm could be assigned to
266 resonances of Gro-2-CH (D-Ala), D-Ala- β H and D-Ala- α H, respectively. These resonances decreased
267 significantly and shifted, indicating a release of D-Ala from the GroP polymer. According to the NMR
268 results, about 70% of the D-alanyl esters were removed by treatment of *B. subtilis* 168 LTA in borate
269 buffer at pH 8 for 24 h at room temperature.

270 Only very small amounts of GroP were released by GlpQ from LTA extracted from wild-type or
271 $\Delta csbB$ mutant cells, AUC of 1.0×10^5 and AUC of 1.8×10^5 were obtained, respectively (**Fig. 5**). The

272 experiment was repeated without preincubation under mild alkaline conditions (borate buffer, pH 8, 24 h),
273 which didn't change the amount of GroP released by GlpQ (Supporting Information, Fig. S3). When
274 incubating the LTA samples under alkaline conditions (0.1 M NaOH, 60°C, 30 min) partial hydrolysis of
275 phosphodiester bonds within the polymer should generate LTA fragments, yet no GroP could be detected,
276 indicating very limited degradation (Figs. 5E and F). Subsequent incubation with GlpQ, however, released
277 substantial amounts of GroP from these LTA preparations, particularly from unglycosylated LTA
278 preparations (Figs. 5G and H). The amount of GroP released by GlpQ was about 3.7-times higher with
279 unglycosylated LTA (AUC = 1.69×10^6) compared to the wild-type LTA (AUC = 4.6×10^5). The same
280 pattern could be observed for LTA obtained from *L. monocytogenes*. While GlpQ released only small
281 amounts of GroP from wild-type (AUC = 6×10^4) and unglycosylated ($\Delta gtlB$) (AUC = 1.2×10^5) LTA
282 (Figs. 6C and D), the amount increased significantly after NaOH pre-treatment (Figs. 6G and H) with about
283 4.2-times as much from unglycosylated LTA (AUC = 1.87×10^6) compared to the wild-type (AUC = 4.5
284 $\times 10^5$). When LTA was pre-treated with NaOH, the LTA polymer was partially cleaved generating smaller
285 fragments. These fragments possess free ends that expose *sn*-glycero-3-phosphoryl groups (Fig. 7).
286 Subsequent digestion of these fragments with GlpQ released significant amounts of GroP. As seen for
287 digestion of WTA by GlpQ, the enzyme was also releasing more GroP from non-glycosylated LTA
288 fragments, as compared to the glycosylated LTA fragments (see Figs. 5 and 6, G compared to H). These
289 results indicate that GlpQ is only able to release significant amounts of GroP from LTA, when the polymer
290 is pre-cleaved with NaOH, generating LTA-fragments. We can only speculate where the low amounts of
291 GroP released by GlpQ from LTA preparation come from. One possibility is that treatment of LTA
292 preparations at pH 8.0 may cause partial phosphodiester cleavage. However, because phosphodiester
293 cleavage under these conditions is unlikely and analysis of the ¹H-NMR spectra of LTA disproves this
294 possibility. Rather, during purification of LTA on a hydrophobic interaction column, lipid II-bound WTA
295 precursors could be co-purified. Since these WTA precursors provide free *sn*-glycero-3-phosphoryl ends
296 the low amount of GroP product released from LTA might come from its degradation.

297 In summary, GlpQ releases GroP in significant amounts from WTA (see Fig. 3), but only very
298 small amounts from LTA preparations (see Fig. 5C and 6C). These findings confirm differences in the
299 stereochemistry of the polyglycerol-phosphate polymers WTA and LTA experimentally. In agreement
300 with the described stereospecificity of GlpQ, WTA consists of Gro3P and LTA consist of Gro1P repeating
301 units. The origin for this difference can be found already in the early stages of biosynthesis. WTA
302 biosynthesis starts with Gro3P, which is transferred to CTP by TagD with the simultaneous release of PP_i,
303 generating CDP-glycerol. The chain polymer is elongated in the cytoplasm with the addition of Gro3P to
304 the growing chain and CMP is released (see Fig. 1A) (53). In contrast, LTA biosynthesis starts with
305 phosphatidylglycerol-CMP, onto which PgsA transfers Gro3P while releasing CMP. The 3P group of

306 Gro3P is released and the product PG is translocated across the membrane and polymerized. The
307 glycerolphosphate group of PG carries a 1-phosphate group, and thus Gro1P is added to the growing
308 chains LTA (see Fig. 1B) (10).

309

310 CONCLUSION

311 This work reveals the distinct stereoisomerism of the glycerophosphate polymers WTA and LTA of *B.*
312 *subtilis* by differential digestion with stereospecific phosphodiesterase GlpQ. Firstly, we showed that the
313 stereospecific *sn*-glycerol-3P phosphodiesterase GlpQ is an exo-lytic hydrolase that sequentially cleaves
314 off GroP entities from WTA, that lack any modification in form of D-alanylation or α -glucosylation, up to
315 the linker unit that connects WTA with the PGN. Secondly, GlpQ is unable to cleave intact, unmodified
316 LTA. Thus, WTA and LTA polymers of *B. subtilis* 168 constitute enantiomers, consisting of Gro3P (WTA)
317 and Gro1P (LTA) building blocks, respectively. Accordingly, limited hydrolysis of LTA with NaOH,
318 which leads to a random cleavage of phosphodiester bonds within the polymer, yields fragments that
319 contain Gro3P terminal ends, from which GlpQ is able to cleave off Gro3P entities. The difference in
320 stereochemistry between the WTA and LTA has critical consequences regarding differential physiological
321 functions, regulation, and turnover of both polymers. The results of this study rationalize the specific
322 interaction of WTA and LTA by stereospecific enzymes and protection against the simultaneous
323 degradation with possibly fatal effects for cell viability.

324

325 Experimental Procedures

326 **Bacterial Strains and Growth Conditions** - The bacterial strains, plasmids and oligonucleotides used in
327 this study are listed in supplemental Table S1. *Bacillus subtilis* 168 wild-type and $\Delta tagE::erm$ strains were
328 obtained from the *Bacillus* genetic stock center (Columbus, Ohio, USA). *B. subtilis* $\Delta csbB::kan$, *Listeria*
329 *monocytogenes* wild-type strain 10403S and $\Delta gltB::strep$ mutant were obtained from the Gründling lab
330 (38). These bacteria were used for the isolation of whole cell wall (peptidoglycan-WTA complex) and
331 teichoic acid preparations. They were cultured at 37°C in lysogeny broth (LB broth Lennox, Carl Roth)
332 with continuous shaking at 140 rpm or on solid LB supplemented with 1.5% agar. Overnight cultures
333 (~16 h) were used to inoculate fresh LB medium and grown to yield an optical density at 600 nm (OD₆₀₀)
334 of 1. Cells were harvested by centrifugation (3000 × g, 20 min, 4°C). *E. coli* BL21 (DE3) cells (New
335 England Biolabs) were used to heterologously express recombinant GlpQ phosphodiesterase from *B.*
336 *subtilis*. These cells, transformed with pET28a-*glpQ*, were grown in LB medium supplemented with 50
337 μg/ml kanamycin until OD₆₀₀ 0.7 was reached, followed by induction with 1 mM isopropyl β-D-

338 thiogalactopyranoside and further propagation for 3 h. Cells were harvested by centrifugation ($3000 \times g$,
339 20 min, 4°C) and used for the purification of recombinant GlpQ.

340
341 **Construction of plasmids and purification of recombinant GlpQ** - *B. subtilis* 168 *glpQ* was amplified
342 by PCR with the primers pET28a-*glpQ*-for and pET28a-*glpQ*-rv (MWG Eurofins, Ebersberg, Germany).
343 Oligonucleotide primers are listed in supplemental Table S1. The PCR products were purified (Gene JET
344 purification kit and Gene Ruler, 1-kb marker, Thermo Fisher Scientific) and then digested with appropriate
345 restriction enzymes (New England Biolabs) and ligated with T4 DNA ligase (Thermo Fisher Scientific)
346 into the expression vector pET28a (Novagen), allowing to overproduce a C-terminal His₆-tag fusion
347 protein. *E. coli* BL21 (DE3) cells carrying pET28a-*glpQ* were grown as described above and lysed in a
348 French pressure cell. The His-tagged GlpQ protein was purified by Ni²⁺-affinity chromatography using a
349 1 ml HisTrap column (GE Healthcare) followed by size exclusion chromatography on a HiLoad 16/60
350 Superdex 200 pg column (GE Healthcare) and purity was checked with a 12% SDS-PAGE. The purity of
351 the enzyme was confirmed via SDS-PAGE (see figure 2 A). From a 1 l culture 3.6 mg GlpQ have been
352 obtained. The enzyme was stored with a concentration of 0.23 mg/ml at -20°C in 0.1 M Tris-HCl buffer
353 (pH 8).

354 **Biochemical Characterization of GlpQ** - To determine the enzymatic properties of GlpQ, 1 pmol of pure
355 recombinant enzyme was incubated with 10 mM GPC. The reaction was stopped by adding 200 μl of pH
356 3.3 buffer (0.1% formic acid, 0.05% ammonium formate) and the released glycerol-phosphate was
357 measured by HPLC-MS. For the pH stability, GlpQ was pre incubated in buffers at different pHs (pH 2:
358 Clarks and lubs, pH 3-6: acetic acid, pH 6-7 MES, pH 7-9: Tris, pH 10: NaHCO₃) for 30 min at 30°C
359 before adding 5 μl each to a 45 μl mix with 0.1 M Tris pH 8 buffer and substrate for 5 min. The pH
360 optimum was tested by incubating GlpQ with 10 mM GPC for 5 min in buffers with different pH. For the
361 temperature stability GlpQ was pre incubated in 0.1 M Tris-HCl, pH 8 at different temperatures ranging
362 from 4 to 75°C for 30 min, followed by a 5 min incubation with GPC at 30°C and pH 8.0. The optimum
363 temperature was tested by incubating GlpQ for 5 min at different temperatures with GPC at pH 8.

364 **Preparation of Cell Wall, WTA and LTA** - For the preparation of cell walls (peptidoglycan-WTA
365 complex) 2 L of *B. subtilis* 168 wild-type or $\Delta\text{tagE}::\text{erm}$ cultures (exponential growth phase, $\text{OD}_{600} = 0.9$)
366 were harvested and resuspended in 30 ml piperazine-acetate buffer (50 mM, pH 6) with 12 U proteinase K
367 and boiled for 1 h. The cytosolic fractions were removed by centrifugation ($3000 \times g$, 15 min, 4°C). The
368 pellet was resuspended in 6 ml buffer (10 mM Tris, 10 mM NaCl, 320 mM imidazole, adjusted to pH 7.0
369 with HCl) and 600 μg α -amylase, 250 U RNase A, 120 U DNase I and 50 mM MgSO₄ were added. The
370 sample was incubated at 37°C for 2 h while shaking, 12 U Proteinase K was added the incubation continued

371 for 1 h. 4% SDS solution was added 1:1 and the mixture was boiled for 1 h. The SDS was removed by
372 repeated ultracentrifugation steps (20 times at 140 000 x g, 30 min, 40°C) and suspension in H₂O_{bidistilled} as
373 well as dialysis against H₂O_{bidistilled}. The SDS content was controlled with the methylene blue assay
374 described earlier (54). The cell wall preparation was dried in a vacuum concentrator.

375 LTA from *B. subtilis* 168 (wild-type and Δ *csbB*) and *L. monocytogenes* 10403S (wild-type and
376 Δ *gtlB*) was prepared by butanol extraction and purification by hydrophobic interaction chromatography
377 using a 24 × 1.6-cm octyl-Sepharose column, according to published protocols (51,52).

378 **Teichoic Acid Digestion with GlpQ and Analysis of Glycerol-phosphate Release** - WTA assays were
379 conducted in 0.1 M Tris-HCl buffer (pH 8, supplemented with 1 mM CaCl₂) with 0.1 mg cell wall
380 preparation (peptidoglycan with attached WTA from *B. subtilis* 168 wild-type and Δ *tagE::erm*) as a
381 substrate and 0.7 μ M GlpQ. The samples were incubated for 30 min at 30°C.

382 LTA assays occurred in 0.1 M Tris-HCl buffer (pH 8, supplemented with 1 mM CaCl₂) with 0.2 mg LTA
383 extract (*B. subtilis* 168 wild-type and Δ *csbB::erm*) and 0.7 μ M GlpQ in a total volume of 50 μ l. The
384 samples were incubated for 1 h at 30°C. LTA was pre-digested by incubating with 0.1 M NaOH for 30
385 min at 60°C, followed by neutralization with HCl and drying in the vacuum concentrator.

386 Sample analysis was conducted using an electrospray ionization-time of flight (ESI-TOF) mass
387 spectrometer (MicrOTOF II; Bruker Daltonics), operated in positive ion-mode that was connected to an
388 UltiMate 3000 high performance liquid chromatography (HPLC) system (Dionex). For HPLC-MS analysis
389 7 μ l of the sample supernatant was injected into a Gemini C18 column (150 by 4.6 mm, 5 μ m, 110 Å,
390 Phenomenex). A 45 min program at a flow rate of 0.2 ml/min was used to separate the compounds as
391 previously described (55). The mass spectra of the investigated samples were presented as base peak
392 chromatograms (BPC) and extracted ion chromatograms (EIC) in DataAnalysis program and were
393 presented by generating diagrams using Python 3.6 with the Matplotlib (version 2.2.2) library.

394

395 **ACKNOWLEDGMENTS**

396 C.M., J.R., and A. P. acknowledge funding by the Deutsche Forschungsgemeinschaft (DFG, German
397 Research Foundation). C.M. receives DFG grants SFB766, Project-ID 398967434 – TRR 261 and Project-
398 ID 174858087 – GRK1708, J.R. receives DFG grant RI 2920/1-1 and A.P. receives DFG grants SFB766,
399 TRR 34 and TRR 156. This work was further supported by the DFG-funded Cluster of Excellence EXC
400 2124 Controlling Microbes to Flight Infections. A.G. acknowledges funding from the Wellcome Trust
401 grant 210671/Z/18/Z and MRC grant MR/P011071/1. The authors declare that they have no conflicts of
402 interest with the contents of this article.

403 **REFERENCES**

404

405 1. Silhavy, T. J., Kahne, D., and Walker, S. (2010) The bacterial cell envelope. *Cold Spring Harb*
406 *Perspect Biol* **2**, a000414

407 2. Armstrong, J. J., Baddiley, J., Buchanan, J. G., Davision, A. L., Kelemen, M. V., and Neuhaus, F. C.
408 (1959) Composition of teichoic acids from a number of bacterial walls. *Nature (London)* **184**, 247-
409 248

410 3. Archibald, A. R., Armstrong, J. J., Baddiley, J., and Hay, J. B. (1961) Teichoic acids and the structure
411 of bacterial walls. *Nature (London)* **191**, 570-572

412 4. Baddiley, J. (1989) Bacterial cell walls and membranes. Discovery of the teichoic acids. *Bioessays*
413 **10**, 207-210

414 5. Schäffer, C., and Messner, P. (2005) The structure of secondary cell wall polymers: how Gram-
415 positive bacteria stick their cell walls together. *Microbiology* **151**, 643-651

416 6. Weidenmaier, C., and Peschel, A. (2008) Teichoic acids and related cell-wall glycopolymers in Gram-
417 positive physiology and host interactions. *Nat Rev Microbiol* **6**, 276-287

418 7. Kohler, T., Xia, G., Kulauzovic, E., and Peschel, A. (2010) Teichoic acids, lipoteichoic acids and
419 related cell wall glycopolymers of Gram-positive bacteria. in *Microbial glycobiology: structures,*
420 *relevance and applications* (Moran, A., Holst, O., Brennan, P., and von Itzstein, M. eds.), Academic
421 press. pp 75-91

422 8. Potekhina, N. V., Streshinskaya, G. M., Tul'skaya, E. M., Kozlova, Y. I., Senchenkova, S. N., and
423 Shashkov, A. S. (2011) Phosphate-containing cell wall polymers of bacilli. *Biochemistry (Mosc)* **76**,
424 745-754

425 9. Brown, S., Santa Maria, J. P., Jr., and Walker, S. (2013) Wall teichoic acids of gram-positive bacteria.
426 *Annual Review of Microbiology* **67**, 313-336

427 10. Percy, M. G., and Gründling, A. (2014) Lipoteichoic acid synthesis and function in gram-positive
428 bacteria. *Annual Review of Microbiology* **68**, 81-100

429 11. De Boer, W. R., Kruyssen, F. J., and Wouters, J. T. (1976) The structure of teichoic acid from *Bacillus*
430 *subtilis* var. niger WM as determined by C nuclear-magnetic-resonance spectroscopy. *European*
431 *Journal of Biochemistry* **62**, 1-6

432 12. Romaniuk, J. A. H., and Cegelski, L. (2018) Peptidoglycan and teichoic acid levels and alterations in
433 *S. aureus* by cell-wall and whole-cell NMR. *Biochemistry*

434 13. Grant, W. D. (1979) Cell wall teichoic acid as a reserve phosphate source in *Bacillus subtilis*. *J*
435 *Bacteriol* **137**, 35-43

436 14. Ellwood, D. C., and Tempest, D. W. (1969) Control of teichoic acid and teichuronic acid biosyntheses
437 in chemostat cultures of *Bacillus subtilis* var. niger. *Biochemical Journal* **111**, 1-5

438 15. Bhavsar, A. P., Erdman, L. K., Schertzer, J. W., and Brown, E. D. (2004) Teichoic acid is an essential
439 polymer in *Bacillus subtilis* that is functionally distinct from teichuronic acid. *J Bacteriol* **186**, 7865-

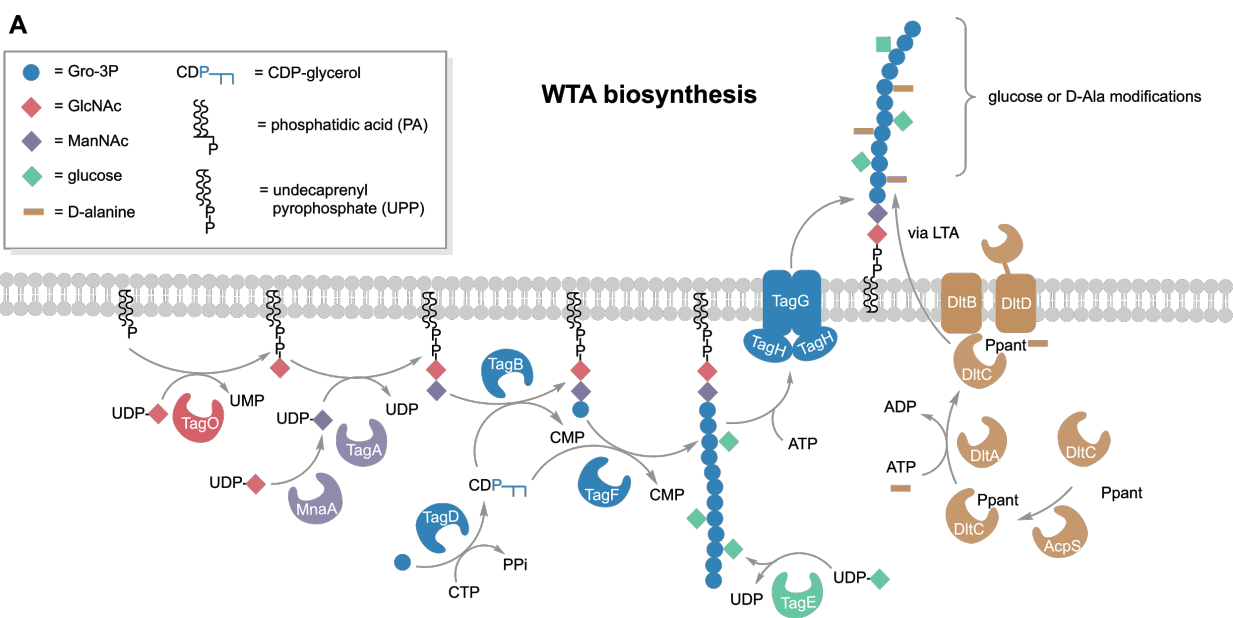
- 440 7873
- 441 16. Ellwood, D. C., and Tempest, D. W. (1972) Effects of environment on bacterial wall content and
442 composition. in *Advances in Microbial Physiology* (Tempest, A. H. R. a. D. W. ed.), Academic Press,
443 London. pp 83-117
- 444 17. Fischer, W. (1990) Bacterial phosphoglycolipids and lipoteichoic acids. in *Glycolipids,*
445 *phosphoglycolipids, and sulfoglycolipids* (Kates, M. ed.), Handbook of Lipid research. pp 123-234
- 446 18. Schirner, K., Marles-Wright, J., Lewis, R. J., and Errington, J. (2009) Distinct and essential
447 morphogenic functions for wall- and lipo-teichoic acids in *Bacillus subtilis*. *Embo J* **28**, 830-842
- 448 19. Xia, G., Kohler, T., and Peschel, A. (2010) The wall teichoic acid and lipoteichoic acid polymers of
449 *Staphylococcus aureus*. *Int J Med Microbiol* **300**, 148-154
- 450 20. Heptinstall, S., Archibald, A. R., and Baddiley, J. (1970) Teichoic acids and membrane function in
451 bacteria. *Nature (London)* **225**, 519-521
- 452 21. Biswas, R., Martinez, R. E., Gohring, N., Schlag, M., Josten, M., Xia, G., Hegler, F., Gekeler, C.,
453 Gleske, A. K., Gotz, F., Sahl, H. G., Kappler, A., and Peschel, A. (2012) Proton-binding capacity of
454 *Staphylococcus aureus* wall teichoic acid and its role in controlling autolysin activity. *PLoS One* **7**,
455 e41415
- 456 22. Morath, S., Geyer, A., and Hartung, T. (2001) Structure-function relationship of cytokine induction
457 by lipoteichoic acid from *Staphylococcus aureus*. *J Exp Med* **193**, 393-397
- 458 23. Morath, S., Stadelmaier, A., Geyer, A., Schmidt, R. R., and Hartung, T. (2002) Synthetic lipoteichoic
459 acid from *Staphylococcus aureus* is a potent stimulus of cytokine release. *J Exp Med* **195**, 1635-1640
- 460 24. Weidenmaier, C., Kokai-Kun, J. F., Kristian, S. A., Chanturiya, T., Kalbacher, H., Gross, M.,
461 Nicholson, G., Neumeister, B., Mond, J. J., and Peschel, A. (2004) Role of teichoic acids in
462 *Staphylococcus aureus* nasal colonization, a major risk factor in nosocomial infections. *Nat Med* **10**,
463 243-245
- 464 25. Matias, V. R., and Beveridge, T. J. (2008) Lipoteichoic acid is a major component of the *Bacillus*
465 *subtilis* periplasm. *J Bacteriol* **190**, 7414-7418
- 466 26. Bontemps-Gallo, S., Bohin, J. P., and Lacroix, J. M. (2017) Osmoregulated Periplasmic Glucans.
467 *EcoSal Plus* **7**
- 468 27. Pooley, H. M., and Karamata, D. (2000) Incorporation of [2-3H]glycerol into cell surface components
469 of *Bacillus subtilis* 168 and thermosensitive mutants affected in wall teichoic acid synthesis: effect of
470 tunicamycin. *Microbiology* **146**, 797-805
- 471 28. Jorge, A. M., Schneider, J., Unsleber, S., Xia, G., Mayer, C., and Peschel, A. (2018) *Staphylococcus*
472 *aureus* counters phosphate limitation by scavenging wall teichoic acids from other staphylococci via
473 the teichoicase GlpQ. *J Biol Chem* **293**, 14916-14924
- 474 29. van der Es, D., Hogendorf, W. F., Overkleeft, H. S., van der Marel, G. A., and Codee, J. D. (2017)
475 Teichoic acids: synthesis and applications. *Chem Soc Rev* **46**, 1464-1482

- 476 30. Gerlach, D., Guo, Y., De Castro, C., Kim, S. H., Schlatterer, K., Xu, F. F., Pereira, C., Seeberger, P.
477 H., Ali, S., Codee, J., Sirisarn, W., Schulte, B., Wolz, C., Larsen, J., Molinaro, A., Lee, B. L., Xia,
478 G., Stehle, T., and Peschel, A. (2018) Methicillin-resistant *Staphylococcus aureus* alters cell wall
479 glycosylation to evade immunity. *Nature (London)* **563**, 705-709
- 480 31. van Dalen, R., De La Cruz Diaz, J. S., Rumpret, M., Fuchsberger, F. F., van Teijlingen, N. H., Hanske,
481 J., Rademacher, C., Geijtenbeek, T. B. H., van Strijp, J. A. G., Weidenmaier, C., Peschel, A., Kaplan,
482 D. H., and van Sorge, N. M. (2019) Langerhans cells sense *Staphylococcus aureus* wall teichoic acid
483 through Langerin to induce inflammatory responses. *mBio* **10**
- 484 32. Neuhaus, F. C., and Baddiley, J. (2003) A continuum of anionic charge: structures and functions of
485 D-alanyl-teichoic acids in gram-positive bacteria. *Microbiol Mol Biol Rev* **67**, 686-723
- 486 33. Perego, M., Glaser, P., Minutello, A., Strauch, M. A., Leopold, K., and Fischer, W. (1995)
487 Incorporation of D-alanine into lipoteichoic acid and wall teichoic acid in *Bacillus subtilis*.
488 Identification of genes and regulation. *J Biol Chem* **270**, 15598-15606
- 489 34. Reichmann, N. T., Cassona, C. P., and Grundling, A. (2013) Revised mechanism of D-alanine
490 incorporation into cell wall polymers in Gram-positive bacteria. *Microbiology* **159**, 1868-1877
- 491 35. Wood, B. M., Santa Maria, J. P., Jr., Matano, L. M., Vickery, C. R., and Walker, S. (2018) A partial
492 reconstitution implicates DltD in catalyzing lipoteichoic acid d-alanylation. *J Biol Chem* **293**, 17985-
493 17996
- 494 36. Brooks, D., Mays, L. L., Hatefi, Y., and Young, F. E. (1971) Glucosylation of teichoic acid:
495 solubilization and partial characterization of the uridine diphosphoglucose: polyglycerolteichoic acid
496 glucosyl transferase from membranes of *Bacillus subtilis*. *J Bacteriol* **107**, 223-229
- 497 37. Allison, S. E., D'Elia, M. A., Arar, S., Monteiro, M. A., and Brown, E. D. (2011) Studies of the
498 genetics, function, and kinetic mechanism of TagE, the wall teichoic acid glycosyltransferase in
499 *Bacillus subtilis* 168. *J Biol Chem* **286**, 23708-23716
- 500 38. Rismondo, J., Percy, M. G., and Gründling, A. (2018) Discovery of genes required for lipoteichoic
501 acid glycosylation predicts two distinct mechanisms for wall teichoic acid glycosylation. *J Biol Chem*
502 **293**, 3293-3306
- 503 39. Kho, K., and Meredith, T. C. (2018) Salt-Induced Stress Stimulates a Lipoteichoic Acid-Specific
504 Three Component Glycosylation System in *Staphylococcus aureus*. *J Bacteriol*
- 505 40. Rismondo, J., Haddad, T. F. M., Shen, Y., Loessner, M. J., and Grundling, A. (2019) GtcA is required
506 for LTA glycosylation in *Listeria monocytogenes* serovar 1/2a and *Bacillus subtilis*. *bioRxiv preprint*
- 507 41. Myers, C. L., Li, F. K., Koo, B. M., El-Halfawy, O. M., French, S., Gross, C. A., Strynadka, N. C.,
508 and Brown, E. D. (2016) Identification of two phosphate starvation-induced wall teichoic acid
509 hydrolases provides first insights into the degradative pathway of a key bacterial cell wall component.
510 *J Biol Chem* **291**, 26066-26082
- 511 42. Borisova, M., Gaupp, R., Duckworth, A., Schneider, A., Dalugge, D., Mühleck, M., Deubel, D.,
512 Unsleber, S., Yu, W., Muth, G., Bischoff, M., Götz, F., and Mayer, C. (2016) Peptidoglycan recycling
513 in gram-positive bacteria is crucial for survival in stationary phase. *mBio* **7**, e00923-00916

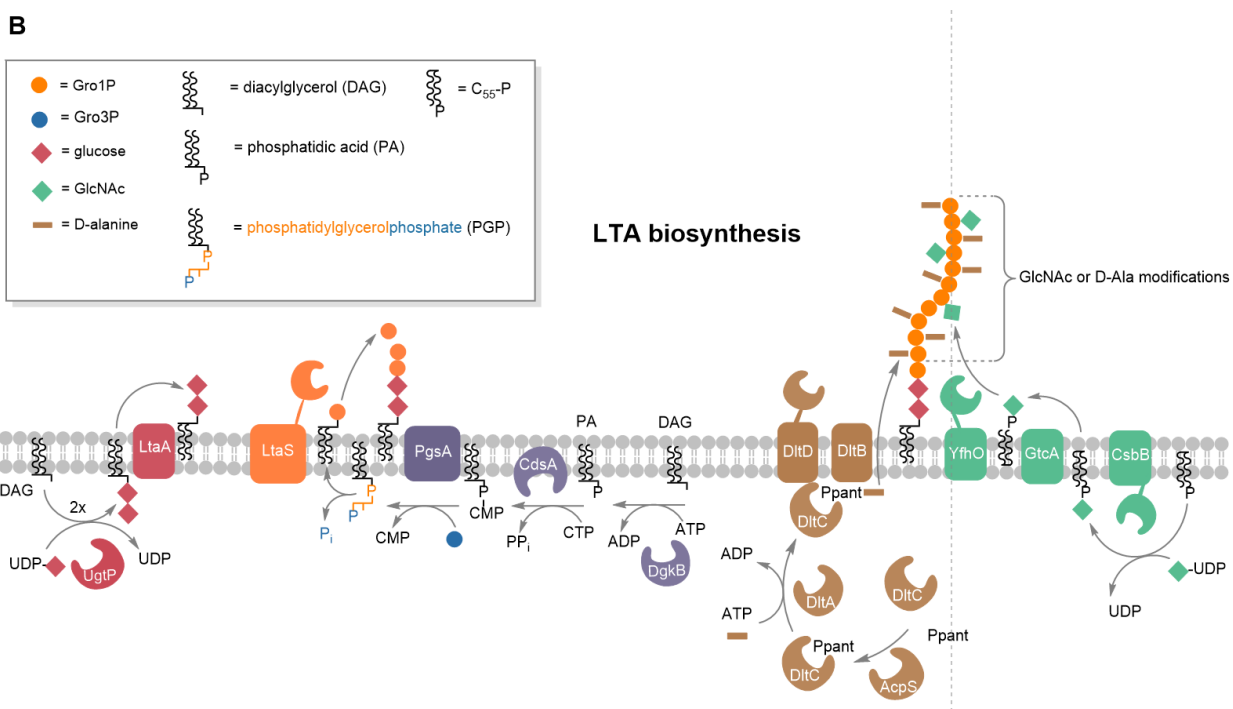
- 514 43. Kluj, R. M., Ebner, P., Adamek, M., Ziemert, N., Mayer, C., and Borisova, M. (2018) Recovery of
515 the peptidoglycan turnover product released by the autolysin Atl in *Staphylococcus aureus* involves
516 the phosphotransferase system transporter MurP and the novel 6-phospho-*N*-acetylmuramidase
517 MupG. *Frontiers in microbiology* **9**
- 518 44. Mayer, C., Kluj, R. M., Muhleck, M., Walter, A., Unsleber, S., Hottmann, I., and Borisova, M. (2019)
519 Bacteria's different ways to recycle their own cell wall. *Int J Med Microbiol* **309**, 151326
- 520 45. Larson, T. J., Ehrmann, M., and Boos, W. (1983) Periplasmic glycerophosphodiester
521 phosphodiesterase of *Escherichia coli*, a new enzyme of the *glp* regulon. *J Biol Chem* **258**, 5428-5432
- 522 46. Larson, T. J., and van Loo-Bhattacharya, A. T. (1988) Purification and characterization of *glpQ*-
523 encoded glycerophosphodiester phosphodiesterase from *Escherichia coli* K-12. *Arch Biochem*
524 *Biophys* **260**, 577-584
- 525 47. Jorge, A. M., Schneider, J., Unsleber, S., Gohring, N., Mayer, C., and Peschel, A. (2017) Utilization
526 of glycerophosphodiesters by *Staphylococcus aureus*. *Mol Microbiol* **103**, 229-241
- 527 48. Shi, L., Liu, J. F., An, X. M., and Liang, D. C. (2008) Crystal structure of glycerophosphodiester
528 phosphodiesterase (GDPD) from *Thermoanaerobacter tengcongensis*, a metal ion-dependent
529 enzyme: insight into the catalytic mechanism. *Proteins* **72**, 280-288
- 530 49. Santelli, E., Schwarzenbacher, R., McMullan, D., Biorac, T., Brinen, L. S., Canaves, J. M., Cambell,
531 J., Dai, X., Deacon, A. M., Elsliger, M. A., Eshagi, S., Floyd, R., Godzik, A., Grittini, C., Grzechnik,
532 S. K., Jaroszewski, L., Karlak, C., Klock, H. E., Koesema, E., Kovarik, J. S., Kreuzsch, A., Kuhn, P.,
533 Lesley, S. A., McPhillips, T. M., Miller, M. D., Morse, A., Moy, K., Ouyang, J., Page, R., Quijano,
534 K., Rezezadeh, F., Robb, A., Sims, E., Spraggon, G., Stevens, R. C., van den Bedem, H., Velasquez,
535 J., Vincent, J., von Delft, F., Wang, X., West, B., Wolf, G., Xu, Q., Hodgson, K. O., Wooley, J., and
536 Wilson, I. A. (2004) Crystal structure of a glycerophosphodiester phosphodiesterase (GDPD) from
537 *Thermotoga maritima* (TM1621) at 1.60 Å resolution. *Proteins* **56**, 167-170
- 538 50. Childs, W. C., 3rd, and Neuhaus, F. C. (1980) Biosynthesis of D-alanyl-lipoteichoic acid:
539 characterization of ester-linked D-alanine in the in vitro-synthesized product. *J Bacteriol* **143**, 293-
540 301
- 541 51. Gründling, A., and Schneewind, O. (2007) Synthesis of glycerol phosphate lipoteichoic acid in
542 *Staphylococcus aureus*. *Proc Natl Acad Sci U S A* **104**, 8478-8483
- 543 52. Percy, M. G., Karinou, E., Webb, A. J., and Gründling, A. (2016) Identification of a lipoteichoic acid
544 glycosyltransferase enzyme reveals that GW-domain-containing proteins can be retained in the cell
545 wall of *Listeria monocytogenes* in the absence of lipoteichoic acid or its modifications. *J Bacteriol*
546 **198**, 2029-2042
- 547 53. Formstone, A., Carballido-Lopez, R., Noirot, P., Errington, J., and Scheffers, D. J. (2008)
548 Localization and interactions of teichoic acid synthetic enzymes in *Bacillus subtilis*. *J Bacteriol* **190**,
549 1812-1821
- 550 54. Hayashi, K. (1975) A rapid determination of sodium dodecyl sulfate with methylene blue. *Anal.*
551 *Biochem.* **67**, 503-506
- 552 55. Gisin, J., Schneider, A., Nägele, B., Borisova, M., and Mayer, C. (2013) A cell wall recycling shortcut

- 553 that bypasses peptidoglycan *de novo* biosynthesis. *Nature chemical biology* **9**, 491-493
- 554 56. Mootz, H. D., Finking, R., and Marahiel, M. A. (2001) 4'-phosphopantetheine transfer in primary and
555 secondary metabolism of *Bacillus subtilis*. *J Biol Chem* **276**, 37289-37298
- 556 57. Ma, D., Wang, Z., Merrikh, C. N., Lang, K. S., Lu, P., Li, X., Merrikh, H., Rao, Z., and Xu, W. (2018)
557 Crystal structure of a membrane-bound O-acyltransferase. *Nature (London)* **562**, 286-290
- 558 58. Reichmann, N. T., and Gründling, A. (2011) Location, synthesis and function of glycolipids and
559 polyglycerolphosphate lipoteichoic acid in Gram-positive bacteria of the phylum Firmicutes. *FEMS*
560 *Microbiol Lett* **319**, 97-105
- 561 59. Wörmann, M. E., Corrigan, R. M., Simpson, P. J., Matthews, S. J., and Gründling, A. (2011)
562 Enzymatic activities and functional interdependencies of *Bacillus subtilis* lipoteichoic acid synthesis
563 enzymes. *Mol Microbiol* **79**, 566-583
- 564 60. Webb, A. J., Karatsa-Dodgson, M., and Gründling, A. (2009) Two-enzyme systems for glycolipid
565 and polyglycerolphosphate lipoteichoic acid synthesis in *Listeria monocytogenes*. *Mol Microbiol* **74**,
566 299-314
567
568
569
570
571
572
573
574
575
576
577
578
579
580
581
582
583
584
585
586

587 **Figure legends**



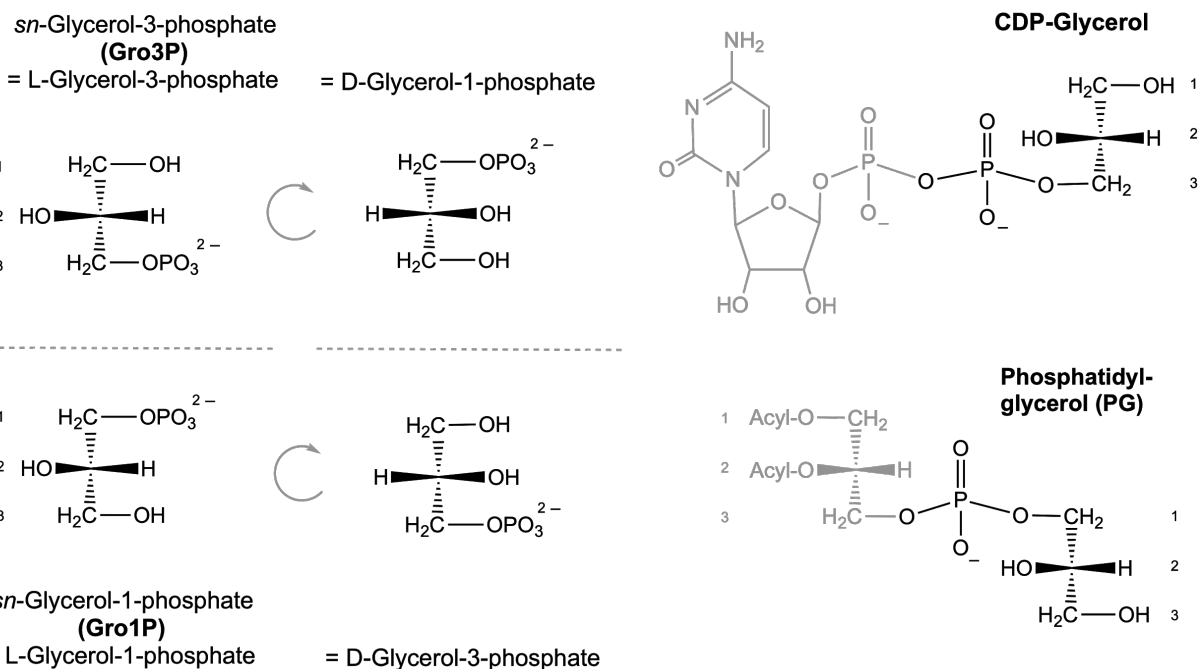
588



589

590

C



591

592

593 **Figure 1. Comparison of the biosynthesis pathways of WTA and LTA and the stereochemistry of**
 594 **glycerol phosphates and teichoic acid precursors**

595 **A**, Overview of WTA biosynthesis. TagO initiates WTA biosynthesis by transferring GlcNAc (red
 596 diamond) from UDP-GlcNAc onto the lipid carrier undecaprenyl phosphate while releasing UMP. MnaA
 597 converts UDP-GlcNAc to UDP-ManNAc, which in turn is used to transfer ManNAc (purple diamond) to
 598 the TagO product, thereby forming the WTA linker disaccharide bound to undecaprenyl pyrophosphate
 599 (UPP). The TagB protein catalyzes a priming step of WTA synthesis in *B. subtilis*, thereby completing the
 600 linkage unit (GlcNAc-ManNAc-Gro3P): a single Gro3P (blue circle) is added from CDP-glycerol (which
 601 is generated by TagD from Gro3P and CTP) to the membrane-anchored linker disaccharide, while releasing
 602 CMP. TagF further elongates the WTA chain polymer by repeatedly transferring Gro3P (blue circles) from
 603 CDP-glycerol. The Gro3P units of the WTA polymer get partially glycosylated in the cytoplasm. The
 604 enzyme TagE utilizes UDP-glucose to attach glucose (green diamonds) onto the C2 hydroxyl group of
 605 Gro3P of the chain polymer. The degree of glycosylation strongly depends on growth conditions and
 606 growth phase. Export of the WTA polymer through the cell membrane is achieved by the ABC-transporter
 607 TagGH. Eventually, the DltABCD system attaches D-alanyl esters to unglycosylated parts of WTA, which
 608 has been reported to occur indirectly via LTA (34). DltA transfers D-alanine in a ATP-dependent two-step
 609 reaction to DltC, which has been modified with 4'-phosphopantetheine (Ppant) at Ser35 by acyl carrier
 610 protein synthase (AcpS) (56). DltB interacts with DltC-Ppant and transfers the D-alanyl onto the C2

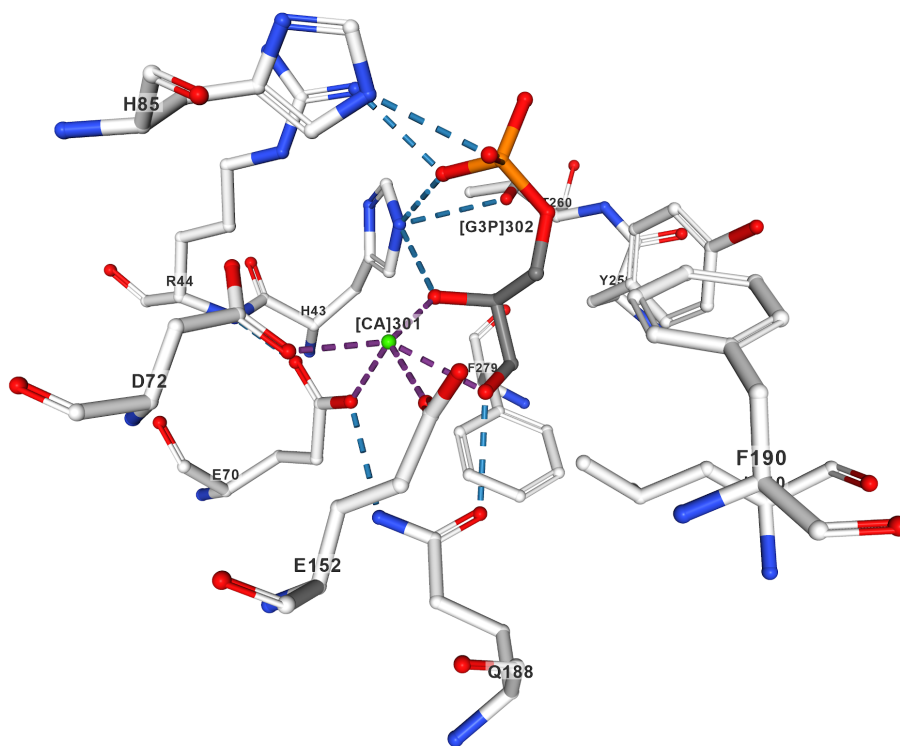
611 hydroxyl group of Gro3P of teichoic acid chains (10,57). **B**, Overview of LTA biosynthesis. The LTA
612 precursor phosphatidyl glycerolphosphate (PGP) is generated by a series of reactions within the cytoplasm.
613 Synthesis starts by phosphorylation of the lipid carrier diacylglycerol (DAG) yielding DAG-phosphate (=
614 phosphatidic acid; PA). The enzyme CdsA then transfers a CMP moiety from CTP onto PA, yielding
615 DAG-CDP while releasing pyrophosphate (PP_i). The CMP moiety of the latter gets exchanged with Gro3P
616 catalyzed by PgsA, thereby forming PGP. Notably, phosphatidylglycerol (PG) is formed by releasing the
617 *sn*-3-phosphoryl group from PGP, thereby retaining a Gro1P entity. It is unknown if this reaction is
618 catalyzed by a so far uncharacterized phosphatase, or if rather the LTA synthase LtaS catalyzes this
619 reaction, in order to energize the polymerisation of Gro1P entities, which are added to the lipid-anchored
620 linker disaccharide in the outer leaflet of the plasma membrane by the housekeeping LTA synthase LtaS_{BS}.
621 The linker disaccharide (red diamonds) is synthesized by UgtP, adding two glucose from UDP-glucose
622 onto DAG. LtaA flips the DAG-linker across the membrane (58). Besides LtaS_{BS}, *B. subtilis* also contains
623 further LTA synthases that catalyse the polymerization of the LTA chains (orange circles): the stress-
624 induced (YfnI) and the sporulation-specific (YqgS) LTA synthase as well as the LTA primase YvgJ, which
625 adds an initial Gro1P to the disaccharide linkage unit (59). LTA polymers may get modified by D-
626 alanylation (brown) and glycosylation (green). As described above alanylation is catalyzed by the Dlt
627 alanylation system: DltA transfers D-alanine to DltC-Ppant and subsequently DltB transfers the D-alanyl
628 onto the C2 of Gro1P (10,57). Glycosylation of LTA is catalyzed by the glycosyltransferase CsbB that
629 adds GlcNAc onto undecaprenyl phosphate (C₅₅-P) using UDP-GlcNAc. As this modification occurs
630 outside the cell in *B. subtilis*, C₅₅-P-GlcNAc is first flipped across the membrane by the flippase GtcA and
631 then the glycosyltransferase YfhO modifies the C2 of Gro1P with GlcNAc (38,40). **C**, The precursors of
632 WTA and LTA synthesis carry enantiomeric glycerol phosphates: *sn*-glycerol 3-phosphoryl (CDP-
633 glycerol) and *sn*-glycerol 1-phosphoryl group (phosphatidyl-glycerol; PG), respectively. Glycerol
634 phosphate enantiomers are defined by convention according to stereochemical numbering (*sn*-
635 nomenclature) as *sn*-glycerol-3-phosphate (Gro3P = L-glycerol-3-phosphate = D-glycerol-1-phosphate)
636 and *sn*-glycerol-1-phosphate (Gro1P = L-glycerol-1-phosphate = D-glycerol-3-phosphate).

637

638

639

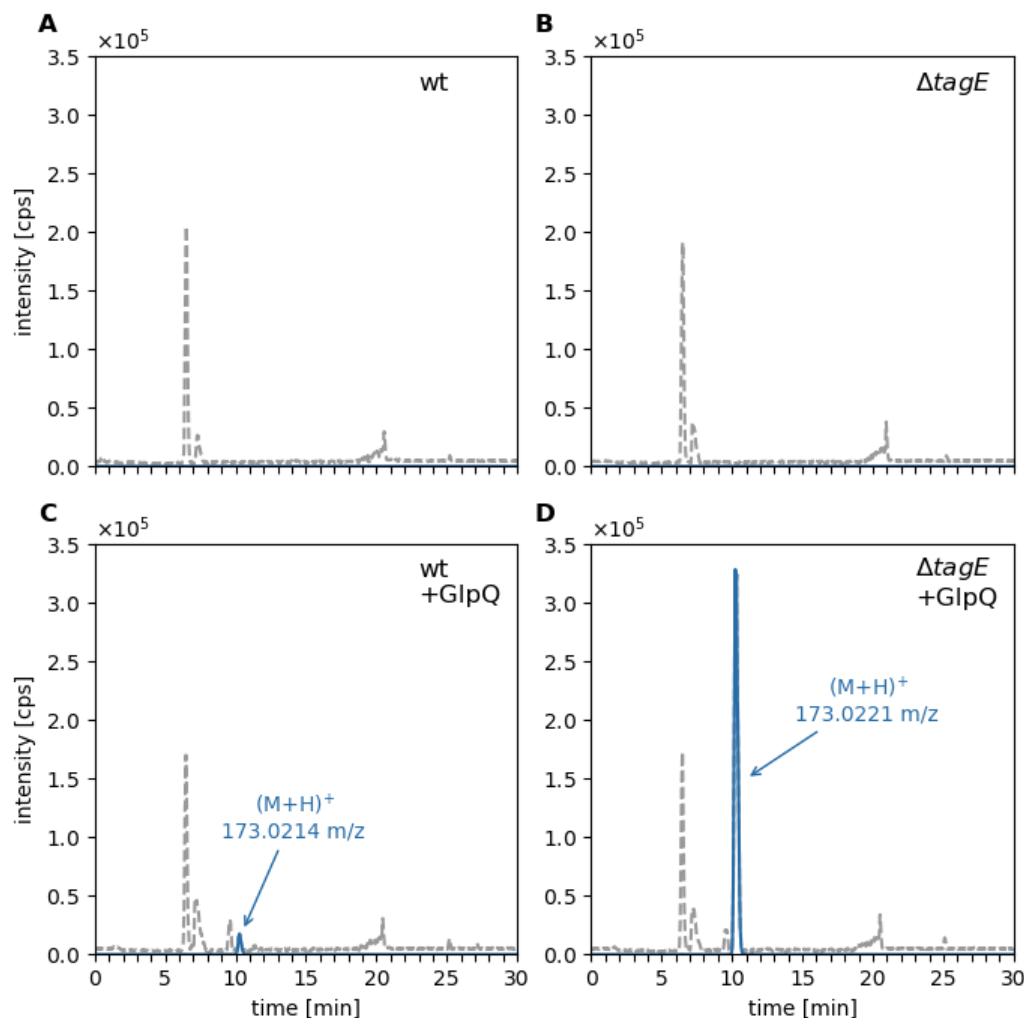
640



641
642 **Figure 2. The co-crystal structure of GlpQ with bound Gro3P (pdb identifier: 5T9B; (41)) rationalizes**
643 **the strict stereospecificity of GlpQ for *sn*-glycero-3-phosphoryl groups.**

644 The active site of GlpQ features a hydrophilic side with His85, His43, Arg44, Asp72, Gln188, Glu152 and
645 Glu70 (left of Gro3P; color code: carbon chains grey; oxygens, red; phosphor, orange, nitrogens, blue).
646 The other side of the binding cleft (right of Gro3P) consists of hydrophobic amino acids like phenylalanine,
647 tyrosine and leucine (Phe190, Tyr259, Phe279). The Ca²⁺ ion adopts a pentagonal bipyramidal coordination
648 and is coordinated by Glu70, Glu152, and Asp72) as well as by the two hydroxyl groups of Gro3P. The
649 phosphate of the Gro3P substrate makes hydrogen bond interactions with Arg44, His43 and His85. The
650 C2 hydroxyl group of Gro3P interacts with Ca²⁺ and His 43 (these interaction would not be possible with
651 Gro1P). Further, the C3 hydroxyl group of the substrate binds to Ca²⁺ and Gln188. The structure
652 rationalizes GlpQ's specificity for *sn*-glycero-3-phosphoryl groups. The C2 hydroxyl group of Gro1P
653 would phase the hydrophobic side and no interaction with Ca²⁺ and His 43 would be possible.

654

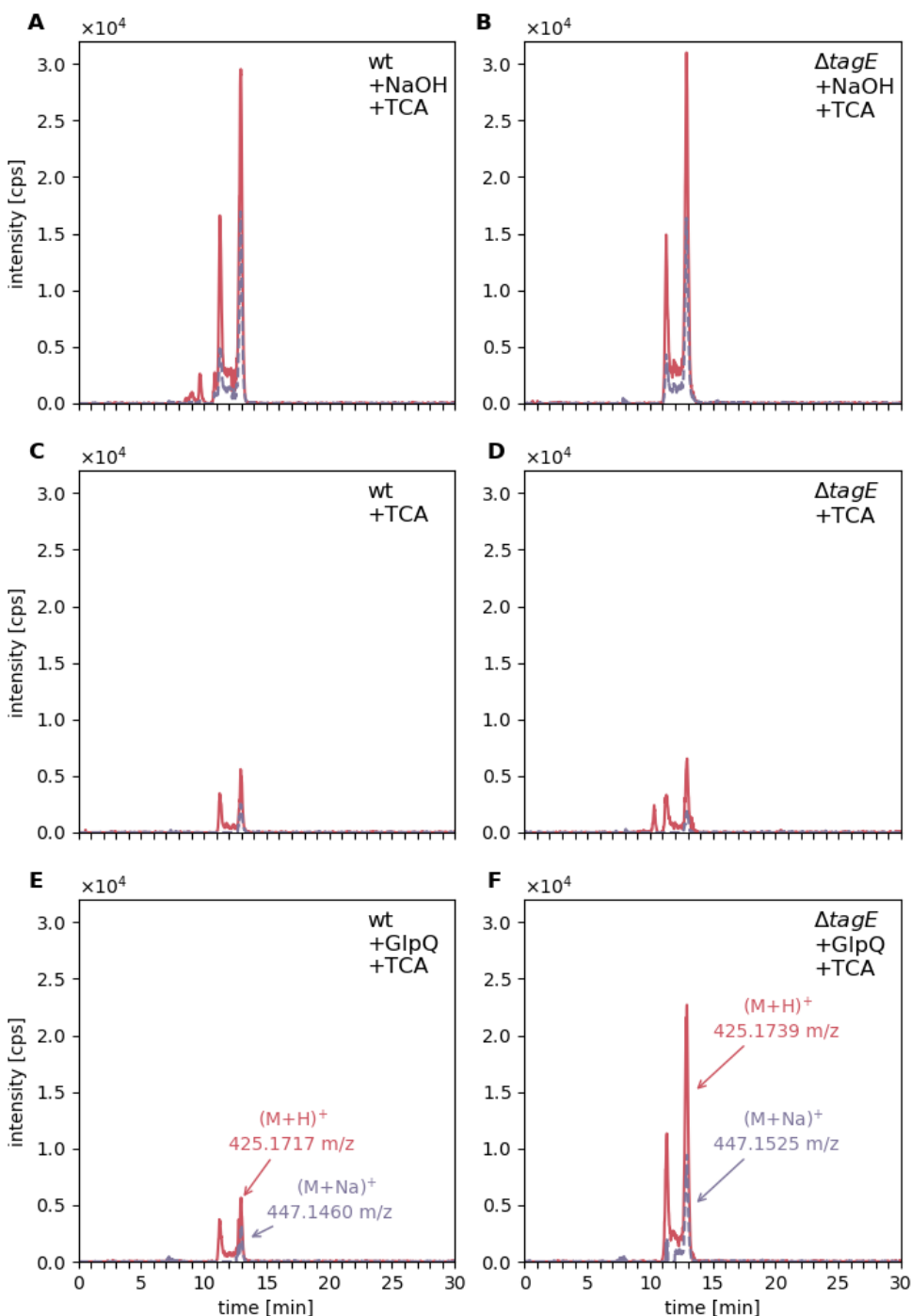


655

656 **Figure 3. GlpQ releases Gro3P from cell walls of *B. subtilis* 168, predominantly from $\Delta tagE$ mutant**
657 **and only little from wild-type (wt) cells.**

658 Purified cell wall of *B. subtilis* (containing peptidoglycan and covalently bound WTA) was incubated with
659 GlpQ and the formation of reaction products was analysed by LC-MS. Shown are the base peak
660 chromatograms (BPC) mass range (M+H)⁺ = 120 – 800 (gray dashed) and the extracted ion chromatograms
661 (EIC) of glycerol-phosphate (M+H)⁺ m/z = 173.022 +/- 0.02 (blue solid). **A**, analysis of wt cell walls
662 (containing partially glycosylated WTA) and **B**, analysis of $\Delta tagE$ cell walls without GlpQ added (control).
663 **C**, analysis of the processing of wt cell walls after incubation with GlpQ for 30 min. The peak area (area
664 under the curve; AUC) of released GroP was AUC = 2.7×10^5 . **D**, analysis of the processing of $\Delta tagE$ cell
665 walls (containing non-glycosylated WTA) digested with GlpQ for 30 min. The obtained AUC = 5.9×10^6
666 was 22 times as much compared to the release of GroP from wt WTA. No glycosylated or alanylated GroP
667 products were detected.

668



669

670 **Figure 4. GlpQ completely digests unglycosylated WTA up to the linker disaccharide ManNAc-**

671 **GlcNAc.** Purified cell wall (PGN-WTA complex; 0.1 mg each) of *B. subtilis* 168 wild-type (wt) and $\Delta tagE$

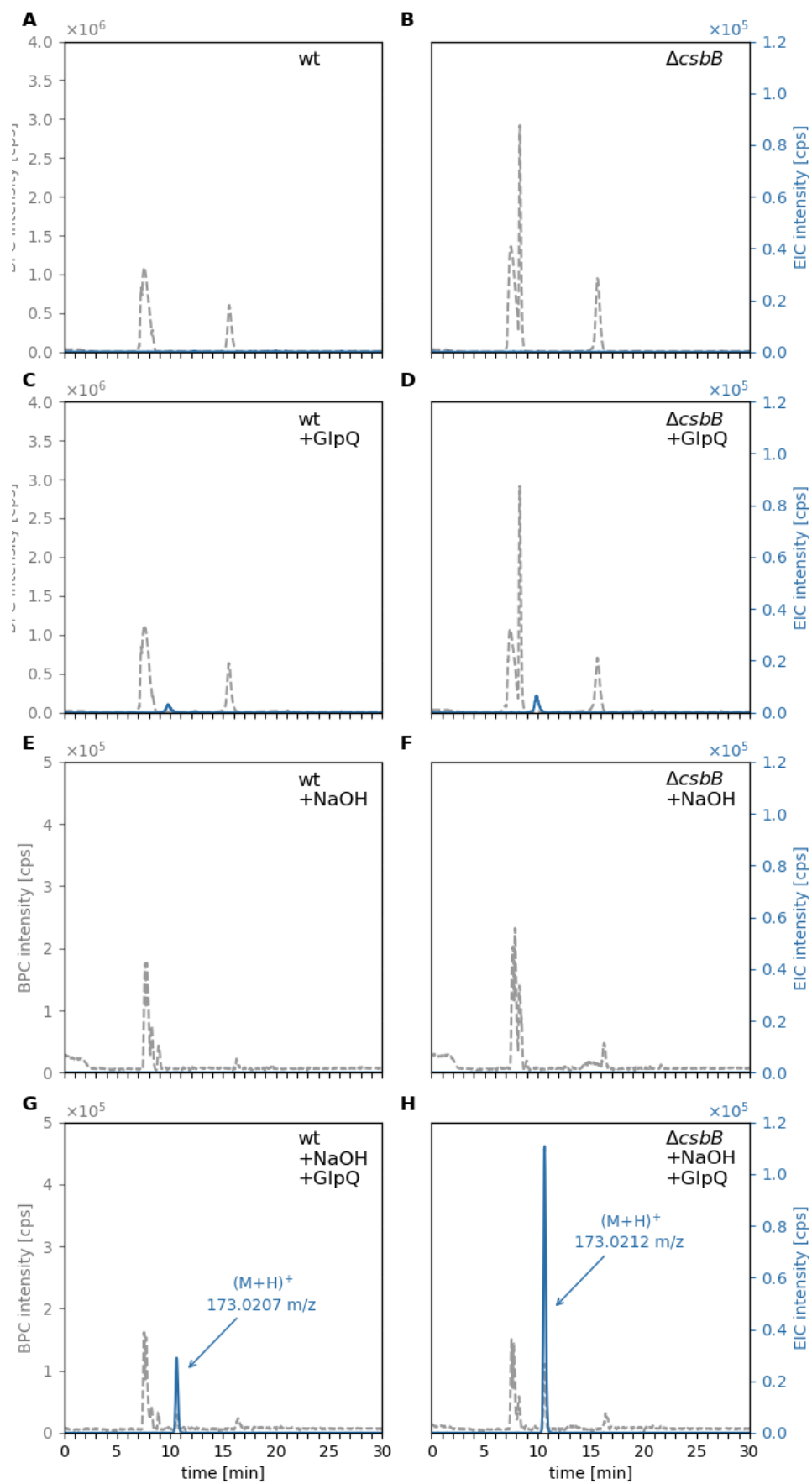
672 was repeatedly incubated with GlpQ (seven times for 10 min at 30°C) following treatment of the remaining

673 substrate with 5 % TCA for 2h at 60°C, cleaving the phosphodiester linkage between PGN and the linker

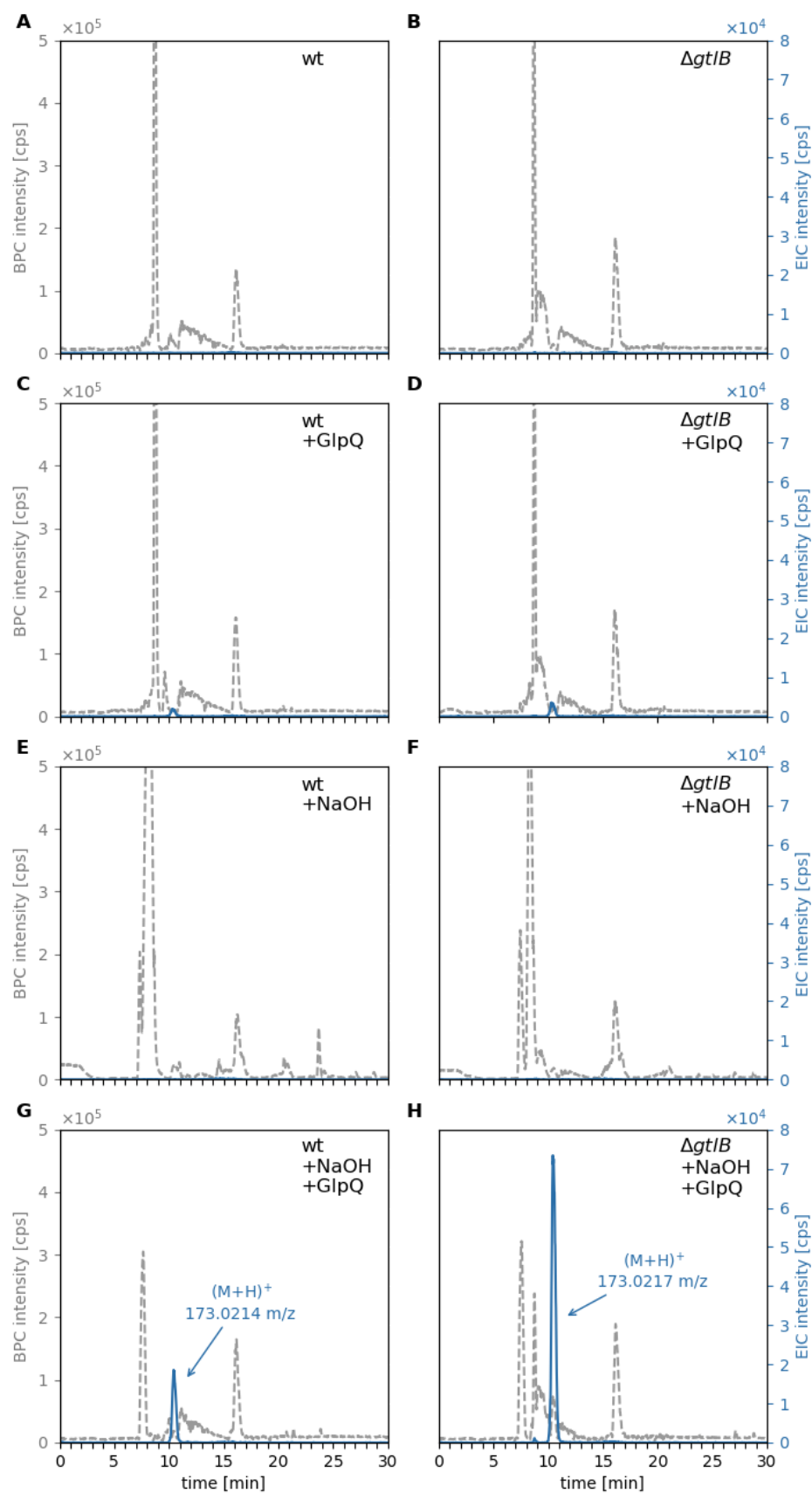
674 disaccharide. The release of ManNAc-GlcNAc was analysed by LC-MS. As a control the cell wall was

675 treated with 0.5 M NaOH for 2h at 60°C to release all GroP from the WTA chain polymers, followed by

676 TCA treatment to release the linker disaccharide. Shown are the extracted ion chromatograms (EIC) of
677 ManNAc-GlcNAc (M+H)⁺ m/z = 425.177 +/- 0.02 (red solid) and (M+Na)⁺ m/z = 447.159 +/- 0.02 (purple
678 dashed). **A** and **B**, complete release of the linker disaccharide after NaOH and TCA treatment from wild-
679 type cell wall (AUC = 15.1 x 10⁵) and from $\Delta tagE$ cell walls containing unglycosylated WTA (AUC =
680 14.8 x 10⁵). **C** and **D**, linker disaccharide released by TCA treatment alone from wild-type cell wall (AUC
681 = 2.38 x 10⁵) and $\Delta tagE$ cell wall (AUC = 3.2 x 10⁵). **E** and **F**, linker disaccharide released by TCA
682 treatment after predigest with GlpQ from wild-type cell wall (AUC = 2.84 x 10⁵, i.e. 3.6 % of total linker
683 disaccharide) and $\Delta tagE$ cell wall (AUC = 1.0 x 10⁶, i.e. 59 % of the totally present linker disaccharide).
684



686 **Figure 5. GlpQ releases *sn*-glycerol-3P from NaOH pre-treated LTA of *B. subtilis* wild-type and**
687 **Δ *csbB* mutant cells.** Purified *B. subtilis* LTA was incubated for 24 h at RT in pH 8 followed by incubated
688 with GlpQ. The formation of reaction products was analysed by LC-MS. Shown are the base peak
689 chromatograms (BPC) mass range $(M+H)^+ = 120 - 800$ (gray dashed) and the extracted ion chromatograms
690 (EIC) of glycerol-phosphate $(M+H)^+ m/z = 173.022 \pm 0.02$ (blue solid). **A** and **C**, wild-type (wt) LTA (=
691 partially glycosylated LTA) incubated without GlpQ (control) with GlpQ. The peak area of released GroP
692 was $AUC = 1 \times 10^5$. **B** and **D**, non-glycosylated Δ *csbB* LTA incubated without GlpQ (control) and with
693 GlpQ. The peak area of released GroP was $AUC = 1.8 \times 10^5$. **E** and **G** wild-type (wt) LTA pre-treated with
694 NaOH incubated without GlpQ (+NaOH) and with GlpQ. The peak area of released GroP was $AUC = 4.6$
695 $\times 10^5$. **F** and **H**, non-glycosylated Δ *csbB* LTA pre-treated with NaOH incubated without GlpQ (+NaOH)
696 and with GlpQ. The peak area of released GroP was $AUC = 1.69 \times 10^6$.



698 **Figure 6. GlpQ releases *sn*-glycerol-3P from NaOH pre-treated LTA of *L. monocytogenes* wild-type**
699 **and Δ *gtlB* mutant cells.** Purified *L. monocytogenes* LTA was incubated with GlpQ and the formation of
700 reaction products was analysed by LC-MS. Shown are the base peak chromatograms (BPC) mass range
701 $(M+H)^+ = 120 - 800$ (gray dashed) and the extracted ion chromatograms (EIC) of glycerol-phosphate
702 $(M+H)^+ m/z = 173.022 \pm 0.02$ (blue solid). **A** and **C**, wild-type (wt) LTA (= partially glycosylated LTA)
703 incubated without GlpQ (control) with GlpQ. The peak area of released GroP was $AUC = 6 \times 10^4$. **B** and
704 **D**, non-glycosylated Δ *gtlB* LTA incubated without GlpQ (control) and with GlpQ. The peak area of
705 released GroP was $AUC = 1.2 \times 10^5$. **E** and **G**, wild-type (wt) LTA pre-treated with NaOH incubated
706 without GlpQ (+NaOH) and with GlpQ. The peak area of released GroP was $AUC = 4.5 \times 10^5$. **F** and **H**,
707 non-glycosylated Δ *gtlB* LTA pre-treated with NaOH incubated without GlpQ (+NaOH) and with GlpQ.
708 The peak area of released GroP was $AUC = 1.87 \times 10^6$.

709

710

711

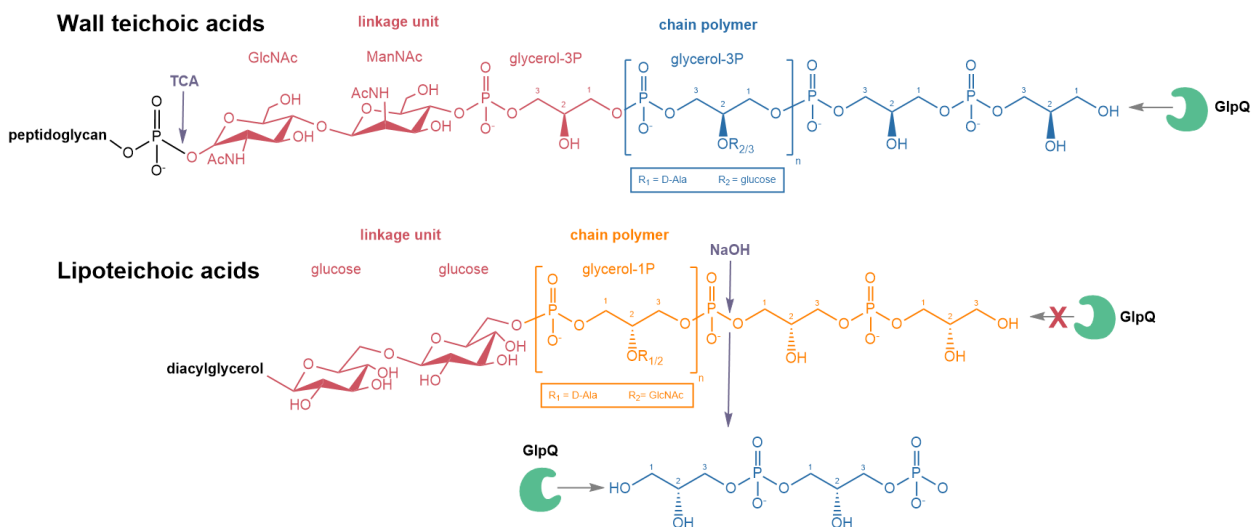
712

713

714

715

716



717

718 **Figure 7. Differential digestion of WTA and LTA with stereospecific *sn*-glycerol-3P**

719 **phosphodiesterase GlpQ.** WTA of *B. subtilis* 168 is phosphodiester polymer made of Gro-3P subunits,

720 that are generally substituted at the hydroxyl group at the C2 position to a certain degree with D-alanine

721 (R₁) or alpha-glucose (R₂). Via a linkage unit (red), consisting of a disaccharide, ManNAc-β(1-4)-GlcNAc,

722 and an unmodified Gro-3P, the WTAs are linked to the C6 of MurNAc of the peptidoglycan via a

723 phosphodiester bond. Using trichloro acetic acid (TCA) the glycosidic phosphodiester bond connecting

724 the WTA linker with the PGN can be cleaved. LTA of *B. subtilis* 168 is a phosphodiester polymer made

725 of Gro-1P subunits, hence represents an enantiomer of the WTA polymer. It can be modified at C2 position

726 with D-alanine or GlcNAc and linked to a diacylglycerol via a glucose-β-1,6-glucose linker disaccharide.

727 GlpQ is able to cleave off Gro-3P from the terminal ends of WTA. Conversely, GlpQ is not able to chip

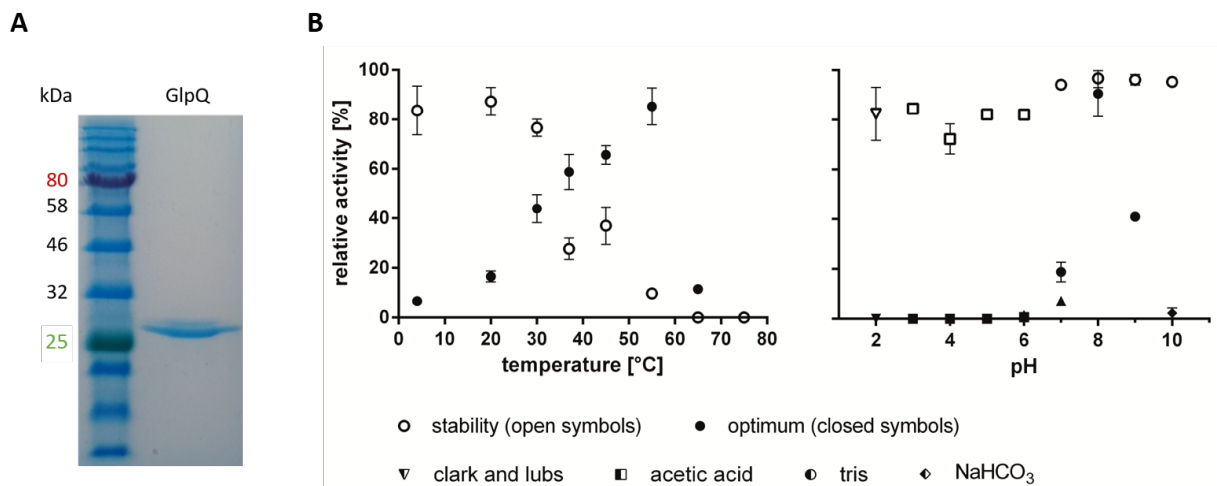
728 off Gro-1P from the terminal ends of LTA. The orientation of the hydroxyl group on the C2 is distinguished

729 by the stereospecific enzyme GlpQ. Treatment with NaOH allows to pre-cleave phosphodiester bonds

730 within the LTA chain polymer, resulting in fragments that contain Gro-3P terminal ends. From these ends

731 GlpQ is able to cleave off Gro-3P moieties. The differential cleavage of WTA and LTA by GlpQ reveals

732 different stereochemistry of the polymers.



733

734

735 **Figure S1. Enzyme purity, stability and optima of recombinant GlpQ.** **A** shows the purity of
736 heterologously expressed recombinant GlpQ-His₆ fusion protein as analysed by SDS-PAGE after
737 purification of the enzyme by Ni²⁺ affinity chromatography and size exclusion chromatography (1 ug
738 protein was loaded on a 12% polyacrylamide gel). A single band is visible just above 25 kDa size marker,
739 in agreement with the calculated molecular weight of GlpQ-His₆ without signal peptide of 29.6 kDa. **B**,
740 shows the temperature and pH characteristics of GlpQ. The enzyme is stable for 30 min at temperatures
741 up to 30°C, but stability rapidly drops at temperatures above 30°C within this time frame. Activity of GlpQ
742 increased with temperature up to 55°C and reveals only about half maximum activity at 30°C. GlpQ is
743 stable within a broad range between pH 2-10 in the indicated buffers and has a very sharp pH-optimum at
744 8.0. In all assays, 1 pmol GlpQ was incubated with 10 mM GPC and reaction product was analyzed by
745 LC-MS, after 30 min of incubation at 30°C. For temperature stability and optimum, 100% relative activity
746 reflect area under the curve (AUC)-values of 2240 and 4088, respectively. For pH stability and pH
747 optimum 100% AUC were 28571 and 31903, respectively.

748

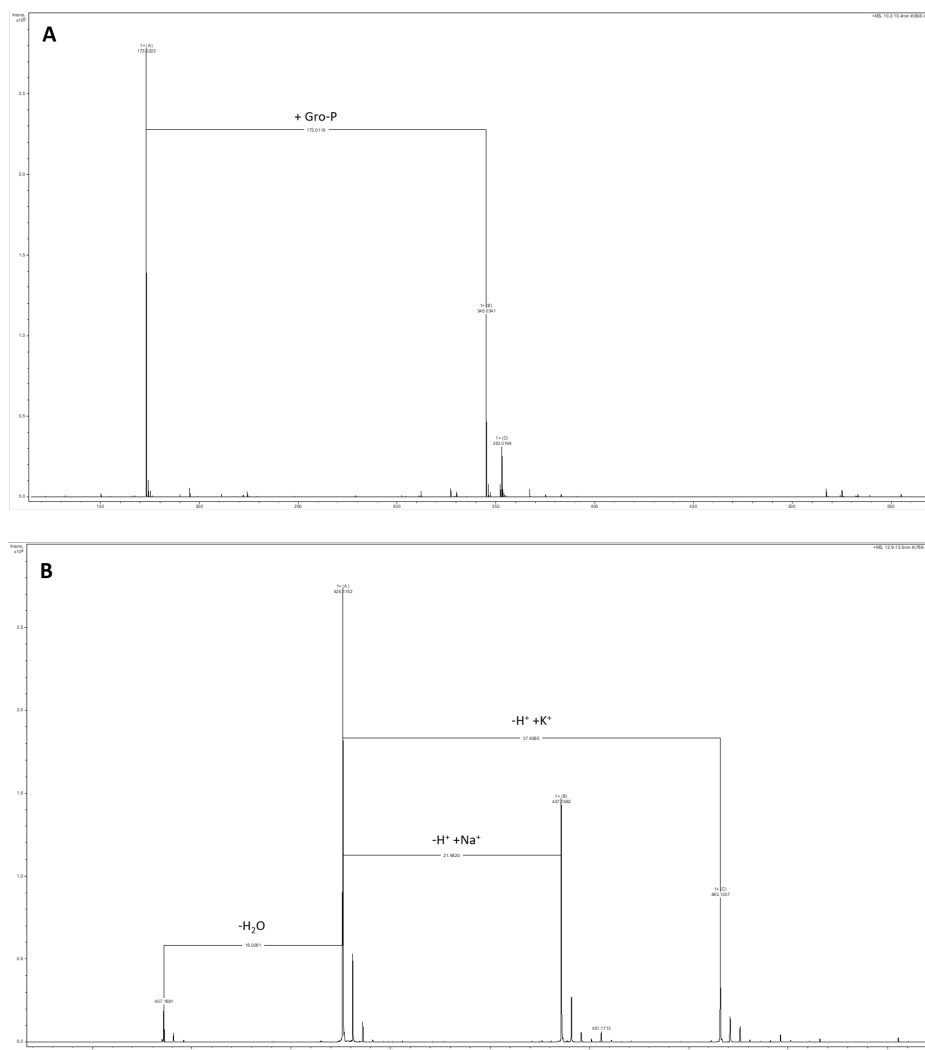
749

750

751

752

753



754

755 **Figure S2. Mass spectra of glycerol-phosphate (GroP) and the WTA linker disaccharide ManNAc-**
756 **β-1,4-GlcNAc.** *A*, shows the mass spectrum of GroP detected in positive ion mode $[M+H]^+$ (experimental
757 173.0222; theoretical monoisotopic mass 173.0210), also revealing a non-covalently bound GroP dimer,
758 $[2M+H]^+$ (experimental 345.0341; theoretical 345.0346). *B*, shows the mass spectrum of the WTA linker
759 disaccharide, ManNAc-GlcNAc, detected in positive ion mode $[M+H]^+$ (experimental 425.1742;
760 theoretical monoisotopic mass 425.1766), also revealing the sodium adduct $[M+Na]^+$ (experimental
761 447.1562; theoretical 447.1585), the potassium adduct $[M+K]^+$ (experimental 345.0341; theoretical
762 345.0346), as well as a product of neutral water loss, $[M-(H_2O)+H]^+$ (experimental 407.1661; theoretical
763 407.1660).

764

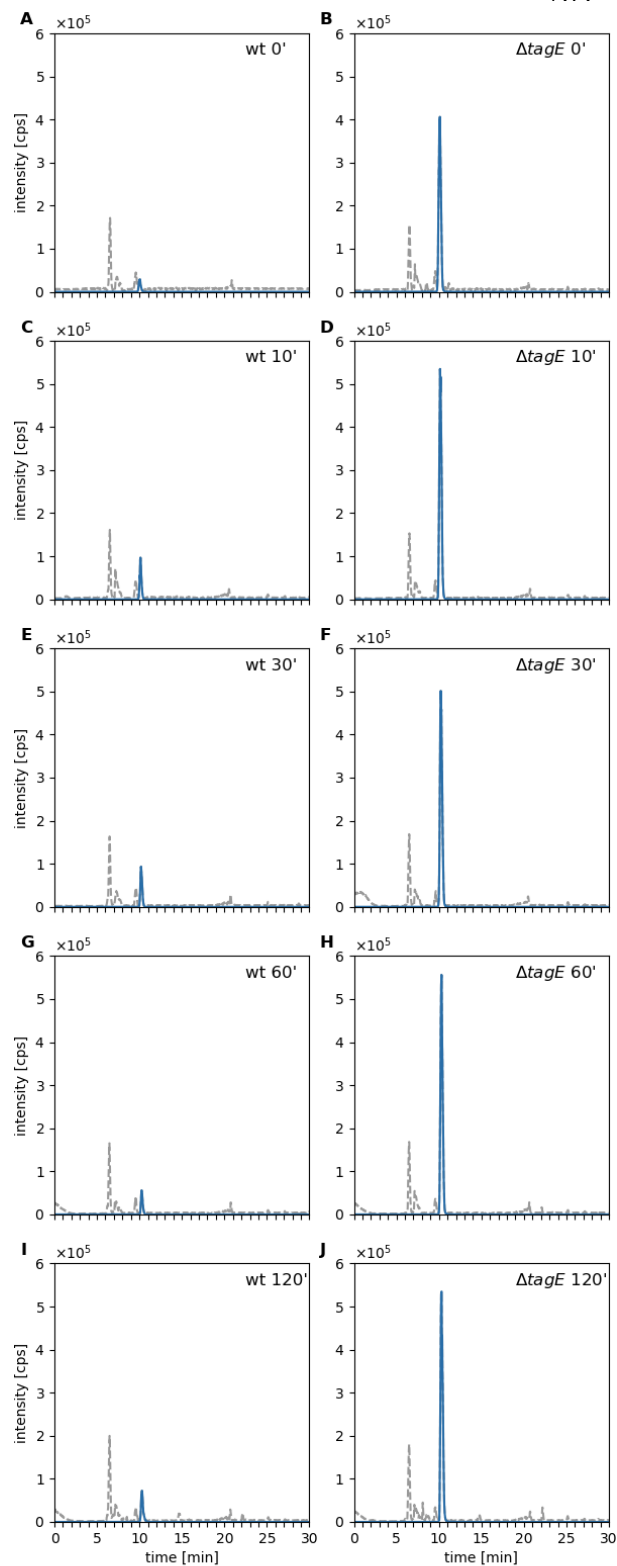
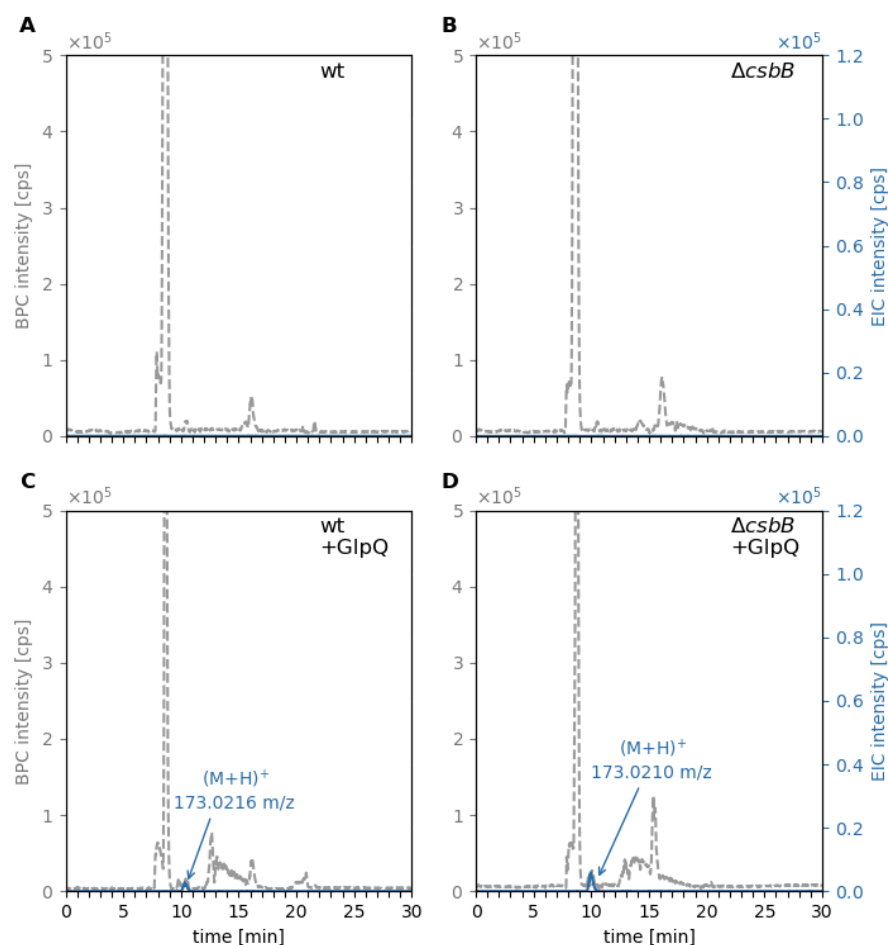
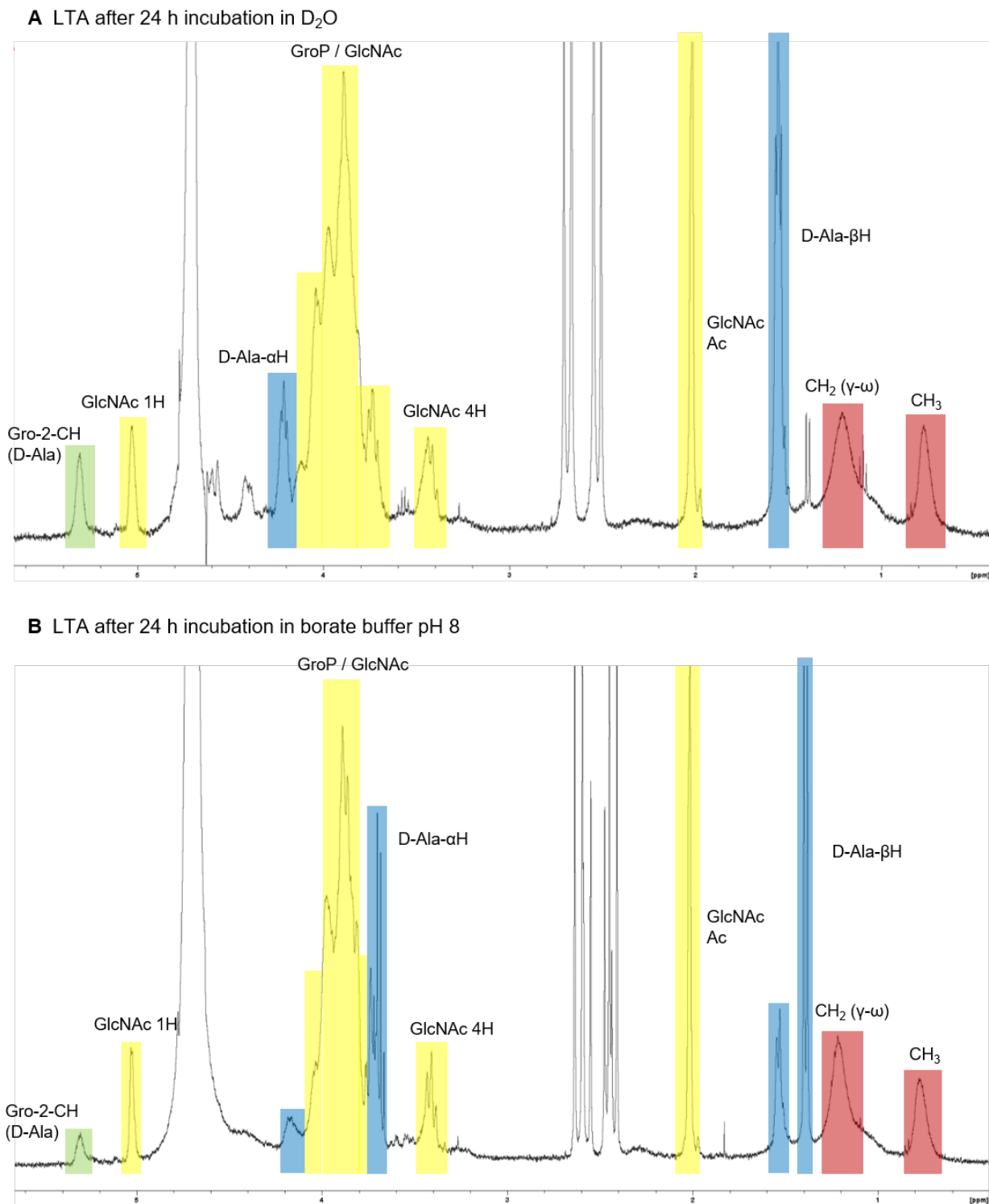


Figure S3. Time course of WTA digest by GlpQ. The vast amount of product (GroP; blue lines) is released by GlpQ within the first seconds of incubation of cell walls purified from wild-type cells (wt; *A,C,E,G,I*; incubation time in min) and unglycosylated cell wall (from *ΔtagE* cells; *B,D,F,H,J*; incubation time in min). GlpQ releases significantly more product from unglycosylated substrate (from *ΔtagE* cells) than from the wild-type. Even over a long period of time on more GroP was released from wild-type cell wall, indicating that GlpQ has only exo- and no endo-lytic activity. 0.25 mg purified cell wall of *B. subtilis* (containing PGN and covalently bound WTA) was incubated with 0.7 μ M GlpQ and the formation of reaction products was analysed by LC-MS. Shown are the base peak chromatograms (BPC) mass range $(M+H)^+ = 120 - 800$ (gray dashed) and the extracted ion chromatograms (EIC) of glycerol-phosphate $(M+H)^+ m/z = 173.022 \pm 0.02$ (blue solid). The reaction was stopped by incubation at 95°C followed by LC-MS analysis.



787

788 **Figure S4. *B. subtilis* 168 LTA not preincubated at pH 8 cannot be cleaved by GlpQ.** Purified *B.*
789 *subtilis* LTA was incubated with GlpQ and the formation of reaction products was analysed by LC-MS.
790 Very little amounts of GroP were released by GlpQ. **A** and **C**, wild-type (wt) LTA (= partially glycosylated
791 LTA) incubated without GlpQ (control) with GlpQ. The peak area of released GroP was $AUC = 6 \times 10^4$.
792 **B** and **D**, non-glycosylated $\Delta cspB$ LTA incubated without GlpQ (control) and with GlpQ. The peak area
793 of released GroP was $AUC = 1.4 \times 10^5$. Shown are the base peak chromatograms (BPC) mass range $(M+H)^+$
794 = 120 – 800 (gray dashed) and the extracted ion chromatograms (EIC) of glycerol-phosphate $(M+H)^+$ m/z
795 = 173.022 \pm 0.02 (blue solid).



796

797 **Figure S5. ¹H-NMR analysis reveals severely reduced D-alanyl ester modifications when LTA was**
798 **incubated for 24 h at pH 8.** Shown are the ¹H-NMR spectra (400 MHz, 303K) of LTA isolated from *B.*
799 *subtilis* 168 wt (2 mg) either incubated for 24 h at RT in D₂O, pH 7.0 **A** or in D₂O containing 0.1 M borate

800 buffer pH 8.0 **B**. Color coding identifies signals indicating removal of D-alanyl residue from the GroP
801 polymer (green): the resonance of the methine group of *sn*-glycerol (Gro-2-CH) containing an D-alanyl
802 ester (D-Ala) is reduced and partially shifted from 5.3 ppm to 3.9 ppm and the D-Ala- α H and D-Ala- β H
803 resonances (blue) are significantly reduced and partially shifted in the LTA sample incubated at pH 8
804 compared to LTA in D₂O. Other resonances assigned to GlcNAc substitution and the GroP polymer
805 (yellow) and to the fatty acids of LTA (red) are not influenced by incubation in borate buffer at pH 8.0.
806 From the signal integrals it was estimated that about two-thirds of the D-Ala substituents were removed
807 in the LTA sample by incubation at pH 8 for 24 h. NMR analysis was performed on a 400-MHz Bruker
808 Advance III spectrometer at 303 K with a TCl cryoprobe. NMR spectra were interpreted according to (22).

809
810
811
812
813
814
815
816
817
818
819
820
821
822
823
824
825
826
827
828
829
830
831
832
833
834
835

836 **Table S1. Strains, plasmids and primer used in the study**

Strain or plasmid	Characteristics	References
<i>E. coli</i>		
BL21 (DE3)	<i>fhuA2 [lon] ompT gal (λ DE3) [dcm] ΔhsdS λDE3 = λ sBamHI ΔEcoRI-B int::(lacI::PlacUV5::T7 gene1) i21 Δnin5</i>	New England Biolabs
<i>B. subtilis</i>		
strain 168 (wild-type)	<i>trpC2</i> ; genome sequenced <i>B. subtilis</i> type strain	<i>Bacillus</i> Genetic Stock Center
$\Delta tagE::erm$	168; <i>trpC2</i> , <i>tagE</i> exchanged by <i>erm</i> ^R with flanking <i>loxP</i> sites	<i>Bacillus</i> Genetic Stock Center
$\Delta csbB::kan$	168; $\Delta csbB::kan$	(38)
<i>L. monocytogenes</i>		
strain 10403S (wild-type)	10403S; StrepR	(60)
$\Delta gtlB::strep$	10403S; $\Delta gtlB$; StrepR	[Rismondo, 2018 #17018]
plasmids		
pET28a	KanR, T7 promoter, ori pBR322, lacI	Novagen
pET28a- <i>glpQ</i>	KanR, T7 promoter, ori, pBR322, lacI, adds C-terminal His ₆ -tag to <i>glpQ</i>	this work
primer		
pET28a- <i>glpQ</i> -for	GATATACCATGGTGGCGTCAAAGGAAACCTGC	this work
pET28a- <i>glpQ</i> -rv	GTGGTGCTCGAGATAACCCTTTTTACTTTGTGGA	this work

837

838